FLUORESCENCE STUDY OF CURCUMIN AND *β*-GLUCAN BINDING INTERACTION: INVESTIGATION OF ITS POTENTIAL AS A QUANTITATIVE METHOD FOR *β*-GLUCAN

BY

PWINT PHYU THEINT

A THESIS SUBMITTED IN PARTIAL FULFILLMENT OF THE REQUIREMENTS FOR THE DEGREE OF
MASTER OF SCIENCE (CHEMISTRY)
DEPARTMENT OF CHEMISTRY
FACULTY OF SCIENCE AND TECHNOLOGY
THAMMASAT UNIVERSITY
ACADEMIC YEAR 2024

FLUORESCENCE STUDY OF CURCUMIN AND β- GLUCAN BINDING INTERACTION: INVESTIGATION OF ITS POTENTIAL AS A QUANTITATIVE METHOD FOR β-GLUCAN

BY

PWINT PHYU THEINT

A THESIS SUBMITTED IN PARTIAL FULFILLMENT OF THE REQUIREMENTS FOR THE DEGREE OF
MASTER OF SCIENCE (CHEMISTRY)
DEPARTMENT OF CHEMISTRY
FACULTY OF SCIENCE AND TECHNOLOGY
THAMMASAT UNIVERSITY
ACADEMIC YEAR 2024

THAMMASAT UNIVERSITY

FACULTY OF SCIENCE AND TECHNOLOGY

THESIS

BY

PWINT PHYU THEINT

ENTITLED

FLUORESCENCE STUDY OF CURCUMIN AND *β*-GLUCAN BINDING INTERACTION: INVESTIGATION OF ITS POTENTIAL AS A QUANTITATIVE METHOD FOR *β*-GLUCAN

was approved as partial fulfillment of the requirements for
the degree of Master of Science (Chemistry)
on June 28, 2024

Chairman _____
(Assistant Professor Kamonthip Seereenonchai, Ph.D.)

Member and Advisor _____
(Associate Professor Jirada Singkhonrat, Ph.D.)

Member and Co-adviser _____
(Siriwit Buajarern, Ph.D.)

Member _____
(Assistant Professor Chitchamai Ovatlarnporn, Ph.D.)

Dean _____
(Associate Professor Supet Jirakajohnkool, Ph.D.)

Thesis Title	FLUORESCENCE STUDY OF CURCUMIN AND *β-GLUCAN* BINDING INTERACTION; INVESTIGATION OF ITS POTENTIAL AS A QUANTITATIVE METHOD FOR *β-GLUCAN*
Author	Pwint Phyu Theint
Degree	Master of Science (Chemistry)
Department/Faculty/University	Chemistry Faculty of Science and Technology Thammasat University
Thesis Advisor	Associate Professor Jirada Singkhonrat, Ph.D.
Thesis Co-Advisor	Siriwit Buajarern, Ph.D.
Academic Year	2024

ABSTRACT

β-glucan from mushrooms gained popularity because of its immune-boosting and anti-tumor effect but its quantitative study was still limited. Currently, available methods have been facing longer analysis time, expensive and unsustainable dyes were involved. In this study, an alternative environmentally friendly fluorescence dye was introduced which is curcumin for the determination of *β*-glucan. Binding occurred by pH-driven method and significant fluorescence enhancement was studied. The influencing factors like temperature, salting effect, pH, the ratio of the fluorophore, and excitation and emission wavelength were optimized to get stable binding interaction. Curdlan was used as a standard for studying linear dynamic range. The consequences will be compared with the existing traditional method of Aniline blue and Calcofluor fluorescence assay. The technique presents a linearity range of 0 to 20 ppm when using 4 ppm curcumin concentration and 20-60 ppm with the 10 ppm curcumin concentration. LOD/LOQ was 0.28/0.92 ppm and 1.5/5 ppm for each curcumin concentration. The method achieved 93-108% recovery with %RSD < 2. *Lentinus squarrosulus* (Herd Khon Khao) and *Lentinula edodes (*shiitake*)* mushrooms were used as a sample and *β*-glucan from these mushrooms was extracted using hot water, alkaline, and microwave extraction.

Keywords: *β*-glucan, curcumin, mushroom, fluorescence, quantification

ACKNOWLEDGEMENTS

First and foremost, I would like to thank my advisor, Associate Professor Dr. Jirada Singkhonrat, for her guidance and support. Her valuable advice, constant encouragement, and steady support have been crucial throughout my research journey.

I also wish to sincerely thank the thesis committee members, mentors, and all the teachers in the Department of Chemistry, Faculty of Science and Technology, Thammasat University. Their expertise and constructive feedback have been invaluable to my studies.

I deeply appreciate the scholarship for talented students provided by the Thammasat International Student Recruitment Program, Thammasat University, under Contract No. TB 2/2565. This financial support has been crucial for my academic endeavors.

Lastly, I am profoundly grateful to my beloved family for their encouragement, inspiration, and steadfast belief in my abilities. I also thank my friends and lab members for their companionship, support, and valuable sharing of knowledge and experiences.

Pwint Phyu Theint

TABLE OF CONTENTS

LIST OF TABLES

LIST OF FIGURES

LIST OF ABBREVIATIONS

Symbols/Abbreviations	Terms
AACC	American Association for Clinical Chemistry
AOAC	Association of Official Analytical Collaboration
AE	Alkaline Extraction
ATR	Attenuated Total Reflectance
C.I.	Color Index
cm	Centimeter
CR3	Complement Receptor 3
Da	Dalton
DMSO	Dimethyl sulfoxide
FDA	Food and Drug Administration
FIA	Flow Injection Analysis
FTIR	Fourier Transform Infrared Spectroscopy
Glucar	Glucan and Curcumin
GRAS	Generally Recognized as Safe
g	Gram
HCl	Hydrochloric acid
HWE	Hot Water Extraction
ICH	International Council for Harmonization
LOD	Limit of Detection
LOQ	Limit of Quantification
Mbar	Millibar
ME	Microwave Extraction
M	Molarity
mM	Milli Molarity
mg/ml	Milligram per milli liter
mg	Milligram
ml	Milli liter

Symbols/Abbreviations	Terms
μM	Micro Molarity
μL	Micro liter
μg	Microgram
n	Number of replicate
nm	Nanometer
MW	Molecular weight
NaCl	Sodium Chloride
Na_2CO_3	Sodium Carbonate
$NaHCO_3$	Sodium Hydrogen Carbonate
NaOH	Sodium Hydroxide
NMR	Nuclear Magnetic Resonance
PAHBAH	p-hydroxybenzoic acid hydrazide
ppm	Part per million
PET	Positron Emission Tomography
Rpm	Revolution per minute
RSD	Relative standard deviation
S	Slope of Calibration Curve
SD	Standard deviation
σ	Standard deviation
λ	Lambda
π	Pi

CHAPTER 1
INTRODUCTION

1.1 Statement of Problem

β-glucan, a type of dietary fiber, possesses rich nutritional and medicinal properties that can be found in the cell walls of various species such as algae, plants, fungi, yeast, and bacteria. It is a biopolymer that has *β*-D glucose units linked together by *β*-glycosidic bonds and is present in various branching degrees including 1-3,1-6 and 1-4 arrangements. Within the COVID-19 pandemic, the *β*-glucan market was reported to be US$523.8 million in 2020 and estimated to reach US$ 868.8 million in 2027 updated by New York Global Newswire. Due to their inherent properties, *β*-glucan plays an important role in various industries such as pharmaceuticals, food, cosmetics, and the brewing industry. The determination of *β*-glucan has gained substantial attention due to several reasons. Firstly, an elevated level of *β*-glucan in human blood indicates a fungal infection enabling early diagnosis. Moreover, *β*-glucan can serve as a quality attribute in the brewing industry, influencing taste grade and viscosity in beer production. Furthermore, several studies have presented the possible use of *β*-glucan as oral formulations in cancer treatment. As a result, the *β*-glucan supplements have been popular, and the implementation of quality control to ensure the effectiveness and safety of these products has been an important measure. *β*-glucan can also be an unwanted contaminant in clinical and pharmaceutical products where the presence of *β*-glucan can compromise the product's performance and safety.

Considering the aforementioned information, the determination of *β*-glucan is essential to ensure product compliance with regulatory standards, suitability and effectiveness of the products, and verification of its quality and purity, for safety, toxicity, and negative impact. Several different determination methods such as enzymatic, chromatography, spectrometry, and electrochemistry have been approached. In the past decades, measurement of *β*-glucan was accomplished through direct and indirect methods which are gravity method and viscosity measurement in indirect way as well as direct measurement of its monomers sugar unit hydrolyzed from

polymeric chains. High-performance liquid chromatography coupled with mass spectrometry; and size exclusion liquid chromatography coupled with light scattering refractive index were also used to analyze *β*-glucan. However, these methods are time and energy-consuming and need experts to operate. To streamline the analysis procedure (McCleary & Codd, 1991). had developed the alternative method which was based on enzyme hydrolysis and had been recognized as standard AOAC method 995.16 so far. However, this reagent is costly, and replicate studies are not feasible. Alternatively, simple spectrometric methods are currently employed in various research to investigate the *β*-glucan content. These presented determination methods so far for *β*-glucan have been facing challenges in terms of cost, specificity, complexity, and time consumption.

Among the various proposed methods, the spectrophotometric method was believed to be the simplest and low-cost economic point of view for the detection of *β*-glucan. Certain types of fluorophores and chromophores such as Aniline blue, Congo red, and Calcofluor that specifically stain *β*-D-glucan have been employed for the determination of *β*-glucan in various samples. However, a few addressed shortcomings are limiting these components to be widely used. In Aniline blue fluorescence analysis, Sirofluor, a contaminant in commercial Aniline blue serves as a fluorophore for fluorescence intensity. Indeed, the length of polymerization and branching degree conformation strongly influence the intensity of fluorescence, and not all species of *β*-glucan can be detected (Gil-Ramirez, Smiderle, Morales, Iacomini, & Soler-Rivas, 2019). Additionally, it is required to stand overnight to decolorize unbound fluorophore which can delay the analysis time (Ko & Lin, 2004). Similar to Aniline blue, Calcofluor is also a widely used fluorophore to examine the *β*-glucan content. It can also specifically and effectively identify *β*-glucan even without a triple helix structure. The drawback of this method is that it relies on several parameters for its successful implementation. It was revealed that the interaction of Calcofluor and *β*-glucan is greatly dependent on ionic strength, molecular weight, pH of buffer solution, and concentration of Calcofluor solution (Kim & Inglett, 2006). Another popular chromophore to bind *β*-glucan was Congo red. It was observed that *β*-glucan in dilute sodium hydroxide solution formed a complex with Congo red where the presence of a hydrophobic interaction was suggested (Nitschke et al., 2011). When Congo red bind

to β-glucan obvious bathochromic shift can be observed from 488 to 516 nm (>20 nm) which has been proved by numerous researchers (Morales et al., 2020; Semedo, Karmali, Fonseca, 2015). Despite the sensitivity, low branching degree β-glucan without a triple helix structure prevents it from expressing the bathochromic shift which suggests Congo red cannot be used in that species (Morales et al., 2020; Semedo et al., 2015). Therefore, it is important to discover new promising fluorophores to develop a simplified and improved detection method at low costs to fill this gap.

Curcumin, bis (4-hydroxy-3-methoxyphenyl)-l,6-heptadiene-3,5-dione, a naturally occurring dye with yellow-orange color gained much attention as a fluorophore because of its promising fluorescence properties, biocompatible and harmless characteristics. Due to its inherent fluorescence properties and keto-enol tautomeric structure, it enables excellent binding to certain molecules and gives sensitive fluorescence responses (Devasena, Balasubramanian, Muninathan, Baskaran, John, 2022) Owing to diverse function groups attached to the main structural unit, curcumin can be involved in various kinds of biochemical interactive pathways by accepting or donating H-bonds. Their π-conjugated systems and β-diketone moiety allow them to present excellent fluorescence emission in certain solvents. Therefore, curcumin has been a valuable tool as a fluorophore in various applications such as in the determination of cysteine, hypochlorite in food samples, and β-amyloid for Alzheimer's disease (Chen et al., 2018; Pang et al., 2017)

Curcumin is a naturally lipophilic compound and numerous studies have reported encapsulating curcumin with β-glucan to be more soluble. It can be loaded with β-glucan by various methods such as incipient wetness impregnation, slurry evaporation, spray drying, and pH-driven methods (Fu et al., 2022; Šalamúnová et al., 2021). Among these methods, the pH-driven method enables a rapid interaction rate. Revealing of strong fluorescence after binding the curcumin and β-glucan has been proved by several studies (Rotrekl et al., 2021; Le et al., 2016). It was observed that the fluorescence intensity was increased after curcumin was loaded onto the β-glucan particles (Le et al., 2016). The fundamental structure of curcumin is highly pH-dependent, and it is a vital tool to control the binding with biological macromolecules like β-glucan. pH-dependent behavior and its aspect on the binding will be studied in this paper.

Among the different sources of β-glucan, this study focuses on the mushroom source because of its well-known immune-boosting activity and antitumor properties. There was limited research on mushrooms like *Lentinus squarrosulus* (Herd Khon Khao) which are abundant in tropical regions while other poplar mushrooms like *Lentinula edodes* (shiitake) mushrooms have been well characterized and analyzed. Therefore, this research includes both mushrooms extracted from three different extraction methods: hot water, alkaline, and microwave extraction. Consequently, the analyzed data by the new method was compared with the known traditional fluorescence method (Aniline blue and Calcofluor). The mushroom β-glucan level ranges from 0.21 to 0.53 % in the low range and 54 to 82 % in the high range depending on the cultivation method, species, specific mushroom body part, and solubility. The current enzymatic assay protocol of AOAC 995.16 detection limit is 1g/100g (1%) and the conventional methods like Aniline blue and Calcofluor method can measure the lower limit of 2 and 0.045 ppm. The objective of this paper aims to explore the binding capabilities of curcumin and β-glucan at different conditions and evaluate their potential as an expedient spectrofluorometric quantification method of β-glucan from the extracts of mushroom samples that offers a rapid and wider linear range at a low cost. Environmentally friendly and greener approaches have gained much attention in recent times to preserve energy, protect natural resources, and reduce negative impacts. Therefore, this study provides an alternative greener approach for sensing β-glucan from mushroom samples in a cost-effective way.

1.2 Research Objectives

- To explore the potential use of curcumin's fluorescence properties in the developing quantification method for the determination of β-glucan.
- To evaluate and optimize the fluorescence measurement condition based on the binding of β-glucan and curcumin for quantification from the extracts of mushroom samples.
- To create a rapid, simplified spectroscopic method that offers a wider linear range.

1.3 Research Scope

- Literature Review and setting the optimization and affecting parameters.
- Extraction of *β*-glucan from *Lentinus squarrosulus* and *Lentinula edodes*
- Optimization of the developed method
- Validation of the developed method
- Comparison with traditional fluorescence methods (Aniline and Calcofluor)

CHAPTER 2
REVIEW OF LITERATURE

2.1 *β*-glucan

β-glucan, a major component of dietary fiber, is a polysaccharide composed of D-glucose monomers linked together by *β*-D-glycosidic bonds. It is mostly found in the cell walls of algae, certain plants, mushrooms, yeast, and bacteria. *β*-glucan structure mostly contains a 1-3-*β*-glucose residue backbone connected by a 1-6 or 1-4-*β*-glucose at different branch points. Composition and conformation vary in branching degrees, patterns of linking, and molecular weight according to their original sources. Mushroom *β*-glucan arranged with 1-6 branch points along linear 1-3 glucose polymer backbone **(Figure 2.1)**. For instance, lentinan from shiitake mushrooms was demonstrated to have two 1-6 *β* branches at every five units of 1-3 *β*-glucan residues (Zhu, Du, Bian, & Xu, 2015). The *β* 1-6 side chain branching degree for yeast *β*-glucan was lesser than mushroom sources (Danielson et al., 2010). Cereal and oat *β*-glucan is a mixed chain of 1-3 and 1-4 D-glucose residues. About 4-8 shorter segments of 1-4 consecutive glucose units appear in specific parts of the main chain (Kim & Inglett, 2006). The primary *β*-glucan structure comprises a random coil, single helix, or triple helix that is dominated by intermolecular bonding, solvent, and temperature of the surroundings (Jin, Li & Wang, 2018). Over 32,000 Da of molecular mass in the chain of *β*-glucan was required to form a triple helix structure (Manabe & Yamaguchi, 2021). Structural diversity and molecular weight from different resources greatly impact their advanced characteristics and therapeutic properties. Mushroom *β*-glucan mainly shows efficacy in anti-tumor and immunomodulating activities. On the other hand, *β*-glucan derived from barley and oat demonstrates effectiveness in lowering blood sugar and cholesterol levels (Zhu et al., 2015).

β-glucan plays a critical role in many application areas and research papers on its beneficial effects have elevated every year. Much research has been reported that consuming *β*-glucan can significantly improve human health (Vetvicka, Vannucci, Sima, & Richter, 2019; Rizkyana et al., 2022). Due to its immune-related activity, *β*-

glucan has become one of the potential dietary supplement regimens for years (Vetvicka et al., 2019). Europe and Asia regions including the United States of America, Canada, Finland, Sweden, China, Japan, and Korea Glucan concede *β*-glucan a stimulating nutraceutical for the immune system (Bashir & Choi, 2017). *β*-glucan particles are strong activators of both acquired and innate immune systems in humans because it is recognized by most of the receptors on the surface of immune cells including macrophages and monocytes particularly dectin 1 and CR3 (complement receptor 3). Empirical evidence demonstrated that the binding of *β*-glucan induced cytokines and antibody production by stimulating the specific immune cells or signaling pathways (Vetvicka et al., 2019). The chain length of monomers, *β* 1-6 branching degrees, and helix conformation exert a substantial impact on the binding of *β*-glucan to immune cell membranes (Manabe & Yamaguchi, 2021). FDA encourages to consumption soluble fiber-rich diet that decreases serum cholesterol levels and subsequently reduces the risk of heart-related disease (FDA,1996).

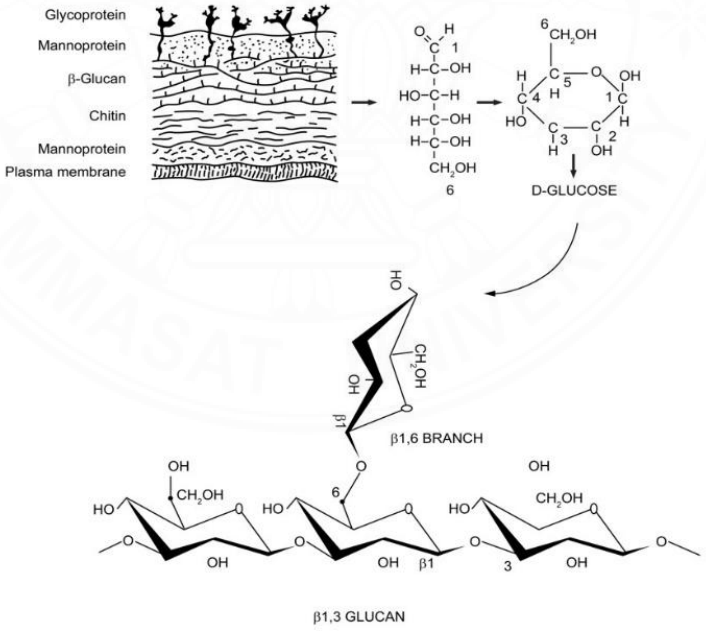

Figure 2.1 *β*-glucan is the main component in the cell wall. The common structure presents *β*-1-3 glycosidic bond with *β*-1-6 branched (Chan, Chan & Sze, 2009).

In addition to its therapeutic characteristics, *β*-glucan is also a valuable marker for diagnostic invasive fungal infections. Traditionally fungal infections were visualized by culturing the affected tissue or blood sample from the patient. However, the risk of taking the sample from a patient with extreme conditions is unbearable and requires the evaluation of alternative non-invasive methods. *β*-glucan was the component of the cell wall of the most infectious fungi Candida spp., Aspergillus spp., and Pneumocystis jirovecii. and can be indirectly determined to investigate the infection (Theel & Doern, 2013; Hammarström, Kondori, Friman, & Wennerås, 2015). The hazardous potential for false positive outcomes in diagnostics corresponding to the contaminants in pharmaceutical products such as wound gauges, hemodialysis apparatus, and blood transfusion equipment should not be negligible (Liss, Cornely, Hoffmann, Dimitriou, & Wisplinghoff, 2015).

Due to its excellent water-holding capacity, emulsifying and gelation properties, and stabilizing emulsion under certain conditions contribute to utilizing it in the food production process. Soluble fibers from cereal-based *β*-glucan are more valuable to employ as food additives. *β*-glucan can be incorporated to elevate loaf and firmness while boosting the content of soluble fiber in the preparation of bread and cake. *β*-glucan can act as an effective thickener in the baking industry due to its enhancing rheological and increasing viscosity incorporated with fat substituent properties. *β*-glucan can also combine with low-fat dairy manufacturing to intensify the gelation and rheological properties (Ahmad, Anjum, Zahoor, Nawaz, & Dilshad, 2012). Beer filtration and quality are strongly influenced by the composition and molecular weight distribution of *β*-glucan. Since the molecular weight of the content of *β*-glucan is related to viscosity and solubilization, the vary in concentration significantly affects the brewing process steps. For instance, the fermentation process alters the *β*-glucan structure and agglomeration behavior, increasing viscosity and promoting adverse effects for the filtration process (Kupetz et al., 2016). There is also a growth of interest into use of *β*-glucan in skin care products for promoting skin health associated with hydration, anti-winkle, revitalization of immune cells, enhanced wound healing and anti-inflammation activity, regeneration of collagen, soothing and antioxidant properties (Du, Bian, & Xu, 2013).

2.2 Current *β*-glucan determination methods

It is a major concern to quantify the content of *β*-glucan in related products and counter-testing for adulteration in quality control management. Numerous methods have previously been studied including enzymatic, chromatography, and spectroscopic detection accompanied by different sample preparation techniques. In 1995, the researchers developed a reversed-phase high-performance liquid chromatographic method for the determination of barley *β*-glucan (Pérez-Vendrell, Guasch, Francesch, Molina-Cano, & Brufau, 1995). This method was not widely popular because it was sophisticated and costly for high-throughput laboratories. Another access was by dissolving the *β*-glucan sample in a DMSO solution and matching the spectra with the standard sample by nuclear magnetic resonance spectroscopic or Flourier transform infrared spectroscopic techniques (Lowman & Williams, 2001). When using these two techniques, all the samples must be soluble in the solvent and involve experts for spectra interpretation. The other approaches relied on absorption and emission spectra either digestion of polysaccharide to detectable monosaccharide (glucose) followed by combination with color-producing substances or direct binding of *β*-glucan structure with specific dye to produce measurable colorant products. The spectrophotometric methods were described in detail as follows in Table 2.1.

2.2.1 Aniline Blue Fluorescence Method

A certain food dye known as Aniline blue (C.I. 42780) was proposed to specifically bind to *β*-D-glucose (Ko & Linn, 2004). The responsible fluorochrome for this reaction is sodium 4,4′-[carbonylbis (benzene-4,1-dial)bis(imino)]bis(benzene sulfonate) which can be seen as impurities of commercially available Aniline blue. The Aniline blue itself does not present fluorescence when dissolved in water or in buffer solution. But when bound with *β*-D-glucan, it presented the fluorescence intensities at 502 nm when excited at 398 nm **(Figure 2.2)**. The specific composition of the dye was essential to achieve the complete binding of *β*-glucan and Aniline blue dye. Since only single helix conformation has the capability of forming the complex with a dye mix, NaOH concentration is also vital to open the triple helix structure of *β*-glucan. This method is the most stable and convenient to examine the *β*-glucan. However, leaving the reagent stock solution overnight is necessary to decolorize the unlabeled

fluorophore. This step is crucial for the removal of residual fluorophores that may interfere with the results. The presence of other polysaccharides in extracts impairs the formation of fluorophore-polysaccharide complexes resulting in disturbance of fluorescence responses. Additionally, this method is not sensitive to β-glucan from some species of mushroom extracts and cannot be applicable as a quantitative method (Gil-Ramirez et al. 2019). Therefore, although the Aniline blue fluorescence method is sensitive enough, the long time to remove residual fluorophore and unable to detect all species render the weakness of this method.

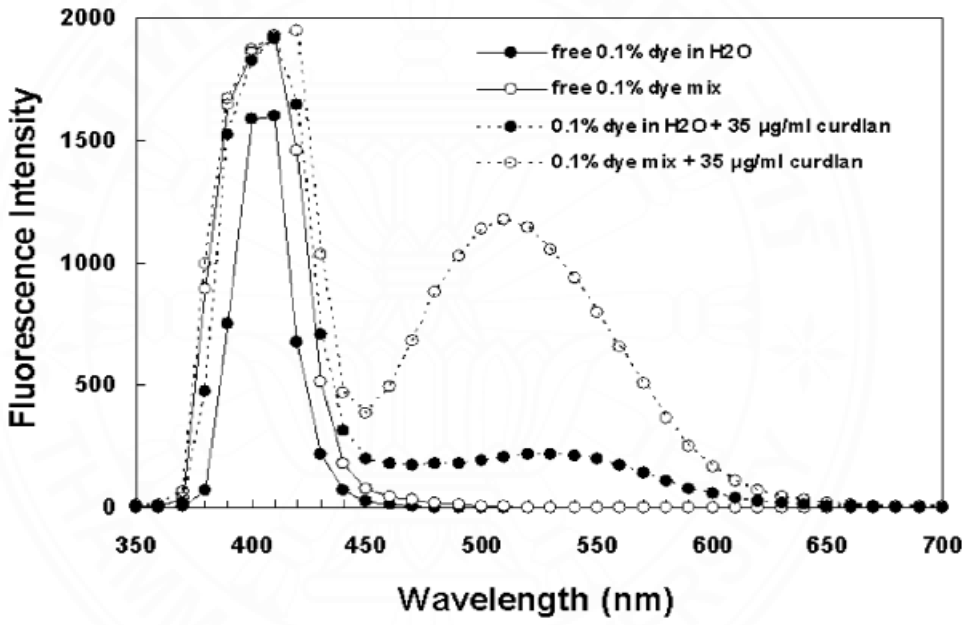

Figure 2.2 Fluorescence spectra of Aniline blue (free form) and Aniline blue and curdlan (β-glucan from bacteria sources) (Ko & Linn, 2004).

2.2.2 Calcofluor Fluorescence Method

It was reported that the consequences of fluorescence intensity when *β*-glucan bound to Calcofluor fluorophore is proportional to the concentration of standard *β*-glucan (Wood et al., 1980). Based on this finding later was developed the flow injection (FIA) method to quantify the *β*-glucan composition in beer and wort plants using Calcofluor as an indicator (Jørgensen, 1983; Mekis, Pintér, Béndek, 1987). To achieve high throughput measurements, numerous modifications have been developed such as flow injection and microplate reader applying Calcofluor as a fluorophore (Kim et al., 2006; Schmitt, Mark, Budde & Allen, 2009). However, this FIA method cannot apply to low molecular weight glucans and strongly depends on ionic strength (Gomez, Navarro, Carbonell & Sendra JM, 2000). Although the FIA method provides high throughput and simplifies the sample processing steps with automation, the instrumental operation costs were not suitable for small laboratory practices. The FIA method was later adapted to a cost-effective microplate assay without scarifying throughput (Schmitt et al. 2009). A relatively large number of experiments can be run in a single microplate, and it is possible to include dilution several times in the microplate reader assay. Regardless of the ease of use, there was a difficulty in pipetting a relatively small number of aliquots 20 μL from beer and wort samples and viscosity was the barrier to flow through the pipette (Schmitt et al. 2009). Furthermore, the Calcofluor method was evaluated to a simple fluorescence spectroscopic method to overcome this gap (Kim et al., 2008).

The shortcoming of this method is that it relies on several parameters for its successful implementation. Fluorescence responses increase by ionic strength and using low ionic strength solution should be avoided. The aggregation was proved by turbidity measurement and the formation was dependent on both the molecular weight of *β*-glucan and the ratio of Calcofluor solution to be used. The aggregation process also interferes with the fluorescence measurement. The precipitation of aggregates can contribute to errors in experiments (Kim et al. 2006). To solubilize and disperse well in the solution, Calcofluor typically requires dissolution in a pH 10 carbonate buffer solution. The hydrogen bonding was found between two entities due to the hydroxyl group from *β*-glucan or Calcofluor and the imine group from Calcofluor. Certain disturbances or interferences can affect the hydrogen bonding

region and consequently, the fluorescence response is diminished. For instance, strong hydrogen bond acceptors such as urea can compete for the binding site with Calcofluor and impair the interaction. Binding efficiency is also affected by several factors such as temperature, ethanol, maltose, NaCl, and buffer concentration (Izawa et al., 1996; Wu et al., 2008). Furthermore, Calcofluor is light light-sensitive fluorophore and preparation must be carried out in dark environments. Indeed, to achieve effective and stable fluorescence intensity, the Calcofluor method must compromise all mentioned factors (Wu, Deng, Tian, Wang, & Xie, 2008).

2.2.3 Congo red UV/Vis Spectroscopic Method

Congo red ($C_{32}H_{22}N_6Na_2O_6S_2$) is an azo dye with a heterocyclic structure primarily intended to stain paper products. It is indicated by the color index (C.I.22120) and exhibits toxic and carcinogenic properties. In both alkaline and weak acid conditions, its color changes to red and expresses a bathochromic red shift while in strong acid, the blue shift occurs. With this excellent characteristic Congo red was applied as a pH indicator formerly (Yakupova, Bobyleva, Vikhlyantsev, & Bobylev, 2019). In 1922, Hans Hermann Bennhold, a physician, accidentally discovered Congo red which is a synthetic dye in the German industry that can stain amyloid (Howie, 2019). Later it was widely used to stain the amyloid β-sheet of Alzheimer's disease (Lendel et al., 2010; Wu, Scott, & Shea, 2012). In 1972, Ogawa tried to complex Congo red with β-glucan in a low alkaline medium. It was found that the affinity of Congo red staining was only specific to the helical conformation of β-glucan. Typically, β-glucan is more soluble in alkaline conditions and less soluble in acidic and neutral pH and can tend to form a gel-like structure. The helical structure is commonly observed in this gel-type β-glucan rather than the random coil. Ogawa demonstrated that at low alkaline pH, the obvious red shift from 489 nm to 520 nm was observed and at a little higher pH no significant shift was found **(Figure 2.3)**. This finding stated that ordered conformation of gel-like β-glucan in a low alkali medium can specifically bind to Congo red dye. The researchers suggested that below 0.25M NaOH concentration was the most favorable condition for the complexation of helical structure β-glucan and Congo red dye (Ogawa, Wanatabe, Tsurugi, & Ono, S, 1972). Although a quantification method to determine β-glucan using Congo red dye was proposed, the application was restricted to only triple helix β-glucan (Nitschke et al., 2011). Nowadays Congo red assay is widely employed

to explore the characterization of triple helix conformation of β-glucan extracted from various sources (Morales et al., 2020; Zhang et al., 2021).

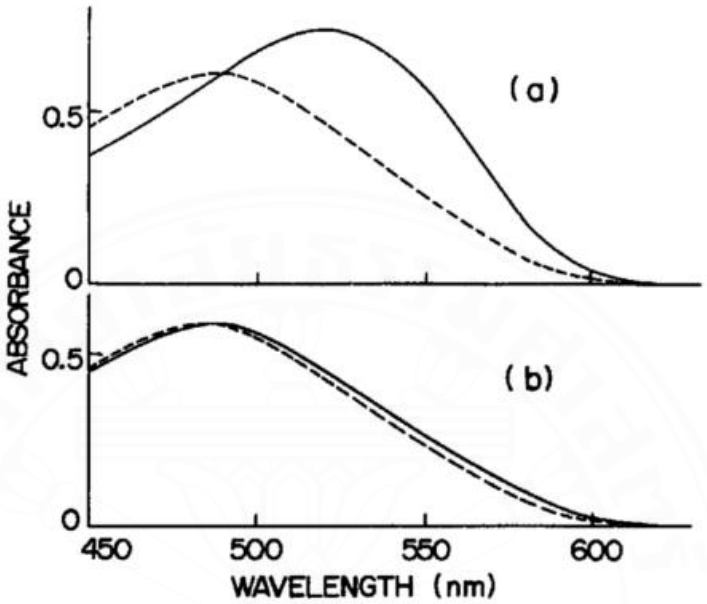

Figure 2.3 The bathochromic redshift of Congo red with (a) low alkaline medium and (b) high alkaline medium (Ogawa et al., 1972).

Table 2.1 The previously reported quantification methods for the determination of *β*-glucan from different sources.

Author	**Method**	***β*-glucan source**	**Mushroom Species**	**Chromophores/ Fluorophores**	**Linear Range** (ppm)	**Dye Concentration**	**LOD** (ppm)
Ko & Linn, 2004	Fluorescence	Six food categories legumes, cereals, tubers, vegetables, fruits, and mushrooms	Shiitake pileus, Snow mushroom, Juda's ear, Mushroom glucan (G5011)	Aniline Blue	0 - 18	0.10%	5
Gil-Ramírez. et al., 2019	Fluorescence	Mushroom	*Auricularia judea, Cantharellus cibarius, Cantharellus tubaeriformis,*	Aniline Blue	0 - 20	0.10%	2

Author	Method	*β*-glucan source	Mushroom Species	Chromophores/ Fluorophores	Linear Range (ppm)	Dye Concentration	LOD (ppm)
			Cantharellus lutescens, Cantharellus cornucopoides, Boletus edulis, Lactarius deliciosus, Pleurotus pulmonarius, Pleurotus eryngii, Morchella conica, Agrocybe aegerita Singer,				

Author	**Method**	***β*-glucan source**	**Mushroom Species**	**Chromophores/ Fluorophores**	**Linear Range** (ppm)	**Dye Concentration**	**LOD** (ppm)
			Amanita caesarea, Hypsizygus marmoreus				
Rieder et al., 2012	Fluorescence	Cereal		Calcofluor	0.1 - 0.4	2 µg/mL	0.045
Schmitt et al., 2009	Fluorescence	Barley		Calcofluor	50 - 250	35 µg/mL	-
Nitschke et al., 2011	UV/Vis	Mushroom (Mycelia)	*Agaricus bisporus* (Button Mushroom) *Flammulina velutipes* (Enoki take)	Congo red	50 - 150	0.08%	5

Author	Method	*β*-glucan source	Mushroom Species	Chromophores/ Fluorophores	Linear Range (ppm)	Dye Concentration	LOD (ppm)
			Grifola frondosa (Maitake) *Hypsizygus tessulatus* (Shimeji Mushroom) *Lentinula edodes* (Shiitake) *Morchella esculenta* (True Morel) *Pleurotus ostreatus* (Oyster Mushroom)				

Author	Method	*β*-glucan source	Mushroom Species	Chromophores/ Fluorophores	Linear Range (ppm)	Dye Concentration	LOD (ppm)
			Pleurotus eryngii (King Trumpet Mushroom) *Pleurotus pulmonarius* (Lung Oyster Mushroom) *Trametes versicolor* (Turkey Tail)				
Semedo et al., 2015	UV/Vis	Mushroom (Fruiting Bodies)	*Ganoderma lucidium, Hericium erinaceus,*	Congo red	0 - 6.0	244 µM	1.51

Author	Method	*β*-glucan source	Mushroom Species	Chromophores/ Fluorophores	Linear Range (ppm)	Dye Concentration	LOD (ppm)
			Coriolus versicolor, Lentinula edodes, Inonotus obliquus, Auricularia auricula, Polyporus umbellatus, Cordyseps sinensis, Agaricus blazei, Poria cocos and Lentinula. edodes				

2.2.4 Enzymatic Method

A lot of scientists have implicated enzyme-related hydrolysis for *β*-glucan determination. Tracing the historical pathways, in 1984 the enzymatic method was developed which applies the *β*-glucanase enzyme to the polysaccharides of glucose molecules. The method first removed endogenous enzymes by dissolving the sample in 80% ethanol and then hydrolyzing it with purified *β*-glucanase enzyme. The resulting sugars were analyzed by reducing sugar assay method where the products were reacted with p-hydroxybenzoic acid hydrazide (PAHBAH) to get a signal. This method required a relatively large amount of enzyme to succeed hydrolysis of all *β*-glucan within the sample (Henry, 1984). Later several approaches using different enzymes were employed. Later the method was evaluated by using lichenase enzyme to hydrolyze *β*-D-oligosaccharides and further break down to glucose molecules by *β*-glucosidase enzyme (Figure 2.4). The hydrolyzed solution was reacted with glucose oxidase/peroxidase reagent solution and incubated at 40°C for 15min to achieve the absorbance for spectroscopic measurement. This method eliminates undesirable interferences as it relies on purified enzymes and is faster than previously described methods that can work 50 samples per day. According to accuracy, precision, and high throughput, it was recognized as AACC Method 32-22 and AOAC Method 995.16.

The drawback of this method was the color development is sensitive to incubation time due to glucose oxidase/peroxidase reagent used. The method was further upgraded and formulated with the reagent mixture named GOPOD reagent. The incubation time was fixed to 20 min at 50°C and the color stability was enhanced for a duration of up to 60 min. Simplified and ease of use reagents result in a high through capability of processing 100-200 samples per day (McCleary & Codd, 1991). Nowadays the reagent is widely commercialized and available as a test kit. Although this method holds great selectivity and efficiency, its applicability was limited to *β* 1-3 and1-4 only. In 2010, this method was expanded to be applicable for *β*-glucan from yeast with the *β* 1-3 and 1-6 branched chains. Liticase enzyme was exerted in replace of lichanse enzyme in this method. All the above-mentioned methods can apply exclusively to physical soft matrices. Sodium hypochlorite Extracting and Enzymatic Digesting (SEED) assay was further reported which was an alternative method to be applicable for hard matrices. They used pancreatin enzyme and ethanol.

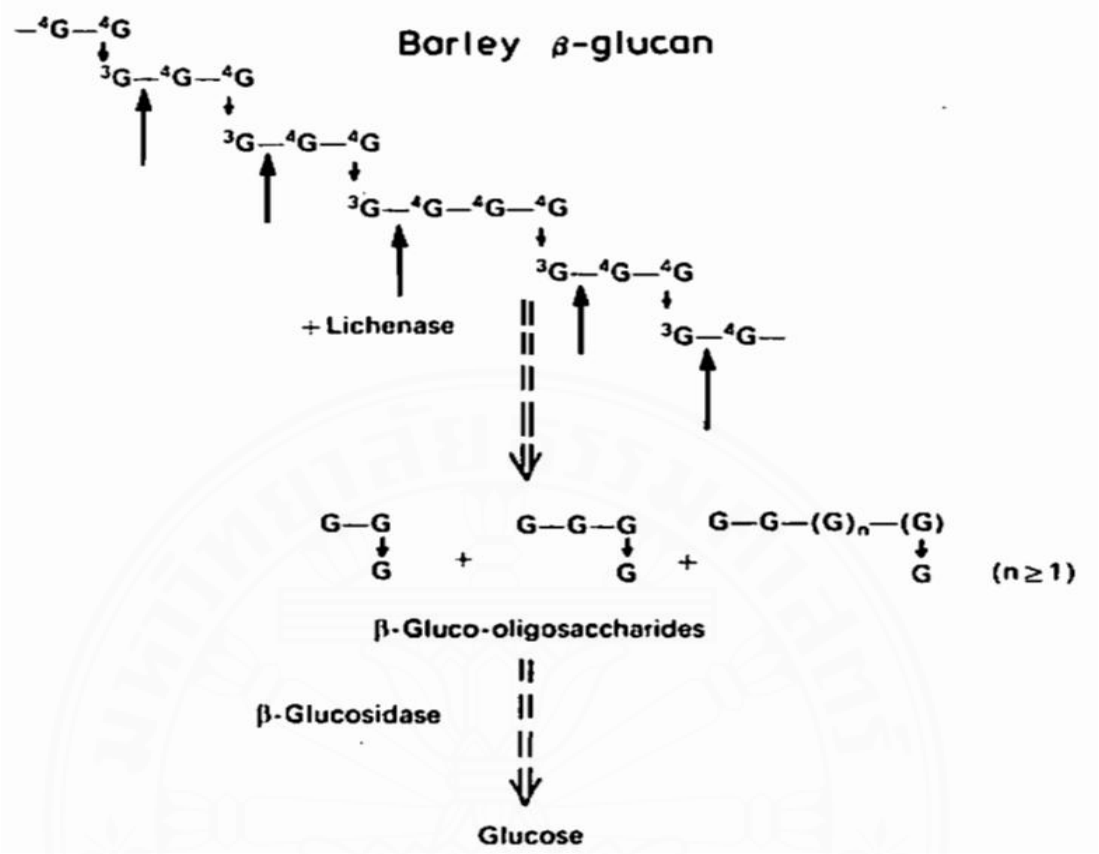

Figure 2.4 Theoretical basis of *β*-glucan assay procedure. (Mcclear et al., 1985)

To take out free sugar and starch and subsequently reduced the strength of the sample by sodium hypochlorite. The *β*-glucan was then dissolved in a DMSO/NaOH solution, and an enzymatic assay was performed similar to AOAC Method 995.16 with some modifications (Ide et al. 2018). Standard protocol (AOAC Method 995.16) was also adapted to the microplate reading system to enhance the throughput. The method was successfully conducted to achieve a wide range of concentrations (0.27-75%) without sacrificing sensitivity and efficiency (Motilva et al., 2014). Nevertheless, the use of direct stain to the *β*-glucan structure was favorable because enzymatic methods are susceptible to interferences of free sugars. These sugars arise from the hydrolysis of starch by an endogenous enzyme called amyl glucosidase and it necessitates removing this enzymatic activity prior to the analysis. In addition, controlling the activity of enzymes from different batches is challenging (Madacsi et al. 1983). Moreover, the method was sample-dependent, and modifications have to be

done in various sample origins (Apostu et al. 2017; Ide et al. 2018) The extensive utilization of the enzymatic method is hindered by the costly production of enzymes and the complex time-consuming procedural steps (Nitschke et al., 2011).

2.3 Curcumin

Curcumin (1,7-bis(4-hydroxy-3-methoxyphenyl)-1-6-heptadiene-3,5-dione), also known as diferuloylmethane presents a natural yellowish-orange color which can be obtained from the rhizome of *Curcuma longa* (turmeric) (Boruah, Saikia, & Dutta, 2012). India and Southeast Asia have used this turmeric powder as a major ingredient for spice in their curries. The plant is also a powerful medicinal herb that remarkedly relieves inflammation and combats various diseases. These properties made it stand out as traditional Ayurvedic medicine in ancient times (Kharat et al., 2017). In addition, curcumin also exhibits antimicrobial, antiparasitic, antioxidant, antimutagenic, and anticancer characteristics. It was not only useful in curry additives and nutraceuticals, but also employed as coloring pigments for food, cosmetics, and textiles. Food and Drug Administration described curcumin as generally recognized as safe (GRAS) components and acknowledged as a safe and non-toxic coloring agent (Kotha, & Luthria, 2019).

Curcumin is a polyphenolic compound constructed with many conjugated double bonds and is chemically hydrophobic in nature (Mabrouk, Hamed, & Mansour, 2021). Curcumin comprises two o-methoxy phenolic groups connected to the α, *β*-unsaturated *β*-diketone (hepta-diene-dione) moiety which can be known as diferuloylmethane ($C_{21}H_{20}O_6$). Structurally it comprises (1) a 7-carbon linker chain, (2) diketone moiety, (3) a phenol ring, and (4) an O-methyl phenolic group **(Figure 2.5)**. The presence of these functional groups contributes curcumin to interact with numerous target compounds. For instance, two adjacent carbonyl groups of methylene in diketone form serve as chelating agents to complex curcumin with metal ions (Khorasani et al., 2019). A strong hydrogen bond was achieved by electro-donating functional groups of hydroxy and methoxy groups linked to phenyl rings of curcumin. Any conditions that can disturb the electronegativity of its group give consequences of lowering hydrogen bonding strength (Devasena et al., 2022). Antioxidant activity can be achieved by phenol groups of curcumin. Conjugated double bonds connected to aromatic rings in

curcumin structure render unsaturated α, β unsaturated carbonyl groups which function as Michael acceptors and are possible for nucleophilic addition (Sahdeo et al., 2021). These properties enable curcumin to interact with proteins, enzymes, and other biomolecules.

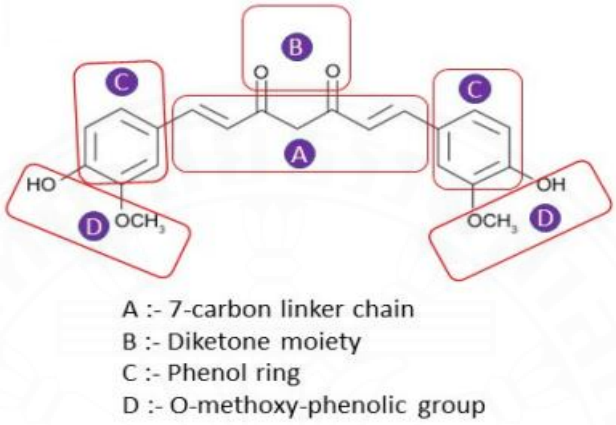

Figure 2.5 Functional groups of curcumin (Sahdeo et al., 2021).

Curcumin can act as a natural fluorophore that presents excellent fluorescence and electrocatalytic properties. It was reported that curcumin can promote the analytical performance of lower sensitivity, specificity, repeatability, reproducibility, and high storage stability when combined with a nano system (Devasena et al., 2022). Due to its keto-enol tautomeric structure, curcumin can bind various biomolecules and nanostructures in different environmental conditions and possess fluorescence, luminescence, UV/Vis absorption, and electrochemical properties. It can display distinct absorption maxima 350 to 480 nm wavelength across different solvation environments (Digambara & Christelle 2011). 360 nm and 428 nm were assigned for the diketo form and keto-enol form respectively and can vary depending on the medium **(Figure 2.6)** (Mabrouk et al., 2021). Curcumin can exhibit fluorescence emission at 538 nm when excited at 420 nm in a polar solvent like ethanol solution (Magdy, Saad Radwan, Belal & Kamal El-Deen, 2023). The spectrophotometric features of curcumin were believed to derive from two aryls butan-2-one structures conjugated by the methylene group. Although the photochemical

nature of these chromophores was not resolved clearly whether it is due to aryl groups or ortho-methyl-phenol groups, modifications or degradation of this structure greatly alters the efficacy of chromophores. Its spectroscopic depends on polar or non-polar solvents and the concentration of interactive components with curcumin (Chignell et al., 1994). The higher fluorescence intensity can be achieved through curcumin dissolved in organic solvents (Karimi et al., 2020). A number of papers that enlightened the solvatochromic properties of curcumin molecules and their dependence on photochemical features have been published (Patra, & Barakat, 2011; Mondal et al., 2016).

UV/Vis and fluorescence spectrophotometry are mainly versatile tools to study the stability, solubility, and tautomeric structural modification of curcumin. The choice of solvent significantly modulates the absorption and emission of energy levels. If a portion of polar solvent was mixed in the aqueous medium, the keto and enol form exhibited in proportion. Degradation kinetics is also affected by the solvent media. When tested with different solvents such as ethanol, isopropanol, ethylene glycol, DMSO and 1, 4 dioxane, maximum stability can be brought off by ethanol (Mondal et al., 2016).

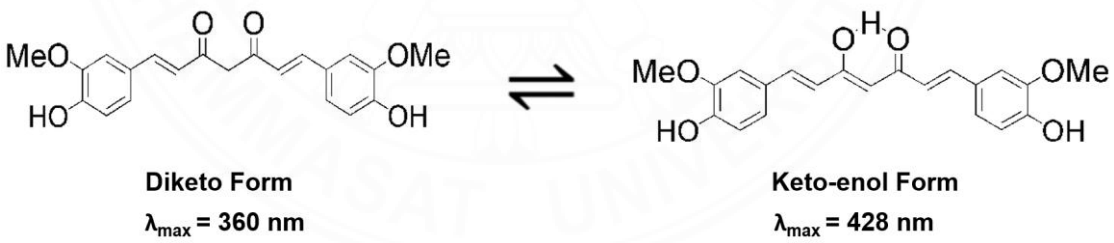

Figure 2.6. Diketo form and keto-enol form of curcumin (Zsila, Bikádi, & Simonyi, 2004).

Due to its excellent fluorescent photophysical properties, curcumin has gained substantial attention as a fluorophore for many applications including bioimaging, biosensors to detect amyloid β-protein, and cancer cells, and can also serve as an ionic ligand for the determination of environmental pollutants such as arsenic, cyanide, and lead. Since curcumin emits fluorescence in the near-infrared region, it has

the benefit of potentially eliminating the risk of interferences from endogenous luminescence from living tissues. Curcumin becomes a versatile tool for bioimaging because of its fluorescence properties, stability, and emission wavelength changes upon binding of the target molecules. One of the popular applications for curcumin as fluorophore was the determination of amyloid *β*-plaques (Aβ plaques; an important factor for diagnosing Alzheimer's disease). Curcumin can bind to insoluble Aβ plaques resulting in a small fluorescent compound that can be detected by positron emission computed tomography (PET) bioimaging (Liu et al., 2021). Moreover, when exposed to environmental pollutants such as cyanide, arsenic, lead, mercury, and fluoride ions, curcumin exhibits an alteration in fluorescence properties. For example, when bound with metal ions, curcumin exhibits a red shift in its absorption spectra. This property can be utilized in various analytical sensing applications of metal ion quantification (Devasena et al., 2022).

2.4 Binding and Fluorescence properties of curcumin and *β*-glucan.

Although curcumin possesses excellent therapeutic properties, low solubility and poor chemical stability in alkaline pH hindered it from being extensively used (Kharat et al., 2017). To form stable molecular complexes, many approaches such as micelles, conjugates, emulsions, liposomes, and hydrogels encapsulate the curcumin molecules. *β*-glucan is one of the potential compounds that can be encapsulated with curcumin and has also been demonstrated to have a synergistic effect in biological and anti-tumor-promoting activities (Le et al., 2016). The interaction with *β*-glucan, the stability, and bioavailability of polyphenols such as curcumin can be improved for implementation in the application of pharmaceuticals, food, and cosmetics (Fang et al., 2021). The soluble level of curcumin in water can be boosted by adding a sufficient level of *β*-glucan particles and enhancing the quality of usage in the food industry. *β*-glucan also provides beneficial effects for the stability of heat and light-sensitive curcumin molecules (Veverka et al., 2014). Apart from being demanded as a food additive, *β*-glucan also serves as the delivery system for upgrading the oral availability and absorption of curcumin in pharmaceutical industries (Plavcová et al., 2019; Le et al., 2016).

To evaluate the binding of *β*-glucan and curcumin compounds, different loading methods have been approached such as incipient wetness impregnation, slurry evaporation method, and spray dry method. However, these conventional loading methods have the disadvantage of prolonging reaction time for one or two days. Currently pH-driven method was proposed which accelerate the reaction time 43.63 fold faster than the previous methods and the loading capacity increased by 5.04 fold (Fu et al., 2022). pH-driven methods are widely employed in food engineering industries for the emulsion process. Hydrophobic curcumin molecules can lose protons from their hydroxyl group in alkaline conditions resulting in an increase of negative charge and favored to accept the proton from *β*-glucan by lowering pH.

Incipient Wetness Impregnation

The stock solution of curcumin 10 mg/ml was dissolved in ethanol and an aliquot of 100µL was added to 100mg of *β*-glucan particles. After gently mixing, the ethanol evaporated out by heating the water bath at 75°C for 4 min. The procedure was repeatedly performed for 30 times to collect a sufficient quantity of curcumin on glucan particles (Šalamúnová et al., 2021)

Slurry Evaporation method

Curcumin was pre-dissolved in 50 ml of ethanol (0.2 mg/ml) and transferred to a 500 ml volumetric flask. 500 mg of *β*-glucan particles were then immersed into a curcumin solution and initiated the combination by a homogenizer. The excess ethanol was evaporated by a rotary evaporator at 175 rpm at 60°C. When all ethanol seemed to dry out, the pressure was adjusted from 1000 to 300 mbar and further reduced to 80 mbar to completely dry out. The resulting yellow fine powder was lyophilized for 2 days and stored in a refrigerator protected from light (Šalamúnová et al., 2021)

Spray Dry Method

Glucan particles were prepared as a suspension (20 mg/ml) and combined with ethanol containing the desired concentration of curcumin compound. The mixture was then fed to a spray dry chamber where the parameters for the operation were; inlet gas temperature-120°C, flow rate-246 l/h, liquid feed flow rate - 5.0 mL/min, and the ultrasonic nozzle power was set to 2.4 W. The outlet gas temperature was 70 ◦C. All

the operation was done under nitrogen atmospheric conditions (Šalamúnová et al., 2021).

pH-driven method

The pH-driven method is not a new method that has been employed for the artificial synthesis of food products in various types such as emulsions, liposomes, and biopolymers. The preparation involves adjusting the pH from alkaline to acidic facilitating the interaction of the molecules by hydrogen bonding and hydrophobic forces. The appropriate amount of β-glucan and curcumin was prepared in 25 ml of 5mM PBS solution (pH 6.5) and 0.1 M NaOH to form a suspension. The mixture was stored at 25°C for 30min in a dark environment. The measured pH was from 12.20 to 12.41 and adjusted back to pH 6.5 with 6M HCl immediately to succeed the reaction. The aliquot was regarded by centrifuging at 15000 xg at 4°C for 10min. The residues of β-glucan and curcumin complex were then freeze-dried at -80°C for further characterization. The color changes after pH driven method can be seen in Figure 2.7 (Fu et al., 2022).

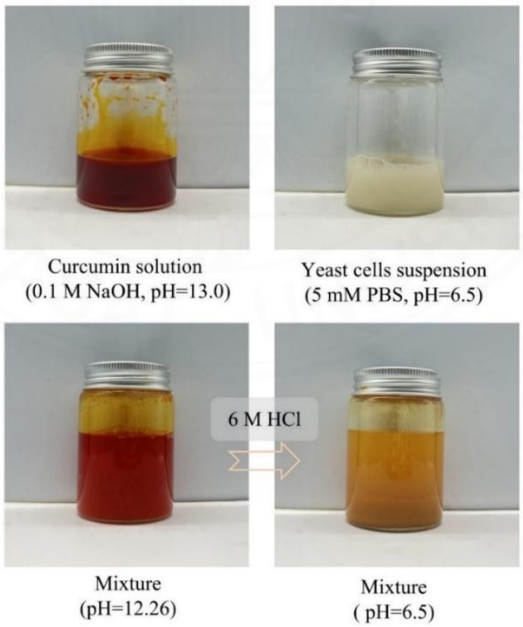

Figure 2.7 Appearance of curcumin color changes during pH-driven method (Fu et al., 2022).

It was demonstrated that the loading capacity and encapsulation efficiency significantly increased (8.07%) and (80.66%) respectively. Moreover, the incubation time for interaction also decreased 43.63 fold when compared to conventional diffusion encapsulation methods. Successive encapsulation was clearly seen as a visual appearance in Figure 2.7 and SEM image in Figure 2.8. There was another experiment that also proved a similar pH-driven method for encapsulation of curcumin in *β*-glucan particles from bacteria sources. (Curdlan from Alcaligenes faecalis) (Fu et al., 2022). Two different *β*-glucan concentrations (Glucar100 is 0.025% curdlan and Glucar 380 is 0.1% curdlan) were examined to confirm their effective binding to the curcumin. It was observed that each size was successful in encapsulation where Glucar 100 achieved 99% loading capacity and Glucar 380 achieved in 100% loading capacity (Figure 2.9). Therefore, pH driven method will be chosen for this study.

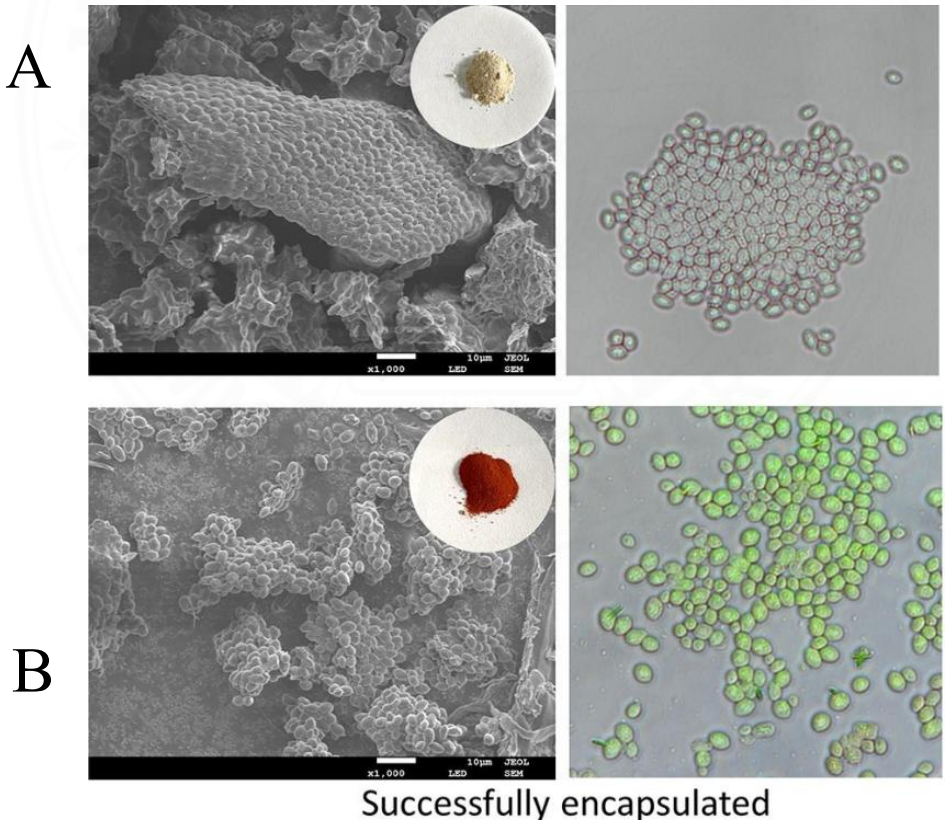

Figure 2.8 SEM micrographs of A. Yeast Cells and B. Curcumin loaded Yeast Cells (Fu et al., 2022).

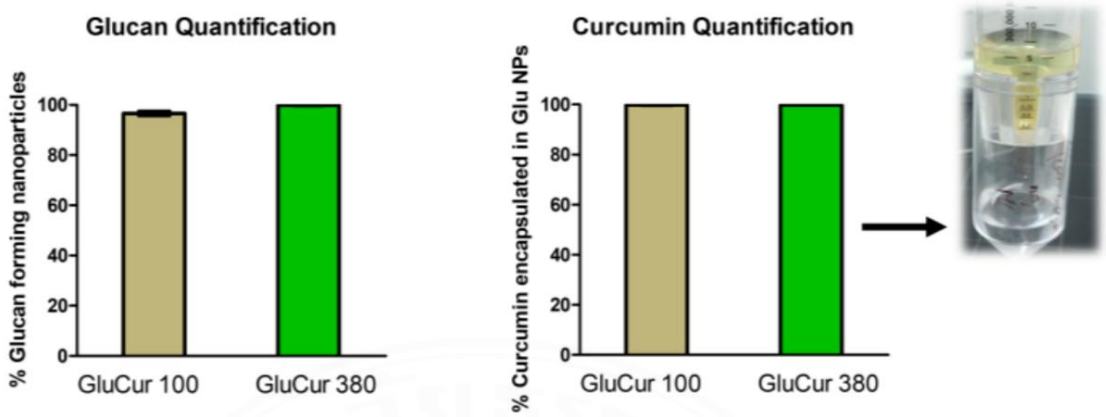

Figure 2.9 Loading Capacity of GluCur 100 and GluCur 380 (Colaço et al., 2023).

Although it was not clearly explained about the interaction of *β*-glucan and curcumin , it was proposed that under alkaline conditions where the pKa of the solution was greater than the enolic and phenolic functional group of curcumin (pKa: 7.8, 8.5, and 9.0), it can render deprotonation resulting in increasing negative charge density, water solubility, and polarity. The mechanism can facilitate their interaction into the wall materials by lowering the pH (Figure 2.10) (Zhan, Dai, Zhang, & Gao, 2020).

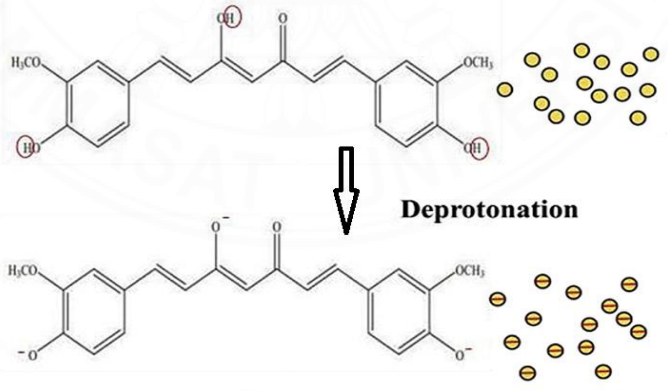

Figure 2.10 Deprotonation of curcumin under alkaline condition (pKa >10) (Zhan et al., 2020)

β-glucan typically exists as a triple helix conformation in aqueous solution. Under certain NaOH concentrations, the *β*-glucan structure can undergo a triple helix

chain opening which facilitates the binding with fluorophore like Aniline blue (Figure 2.11). Therefore, the alkaline condition was supposed to be critical in the binding mechanism.

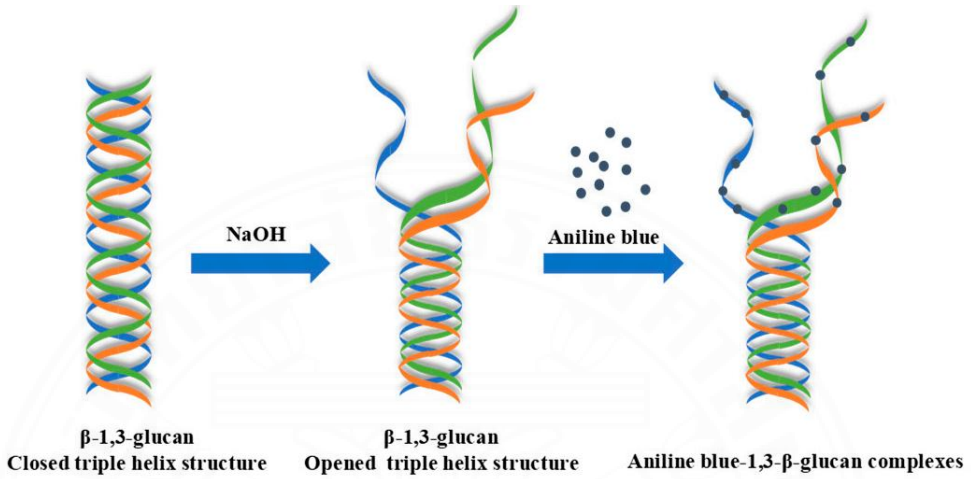

Figure 2.11 Triple helix chain opening of *β*-glucan under certain NaOH concentration (Fu et al. 2019).

The fluorescence nature of *β*-glucan and curcumin binding mechanism have investigated that the fluorescence intensity increased after curcumin has encapsulated with *β*-glucan. However, the absorption as well as emission wavelength shifted ~ 20 nm from its original wavelength suggesting that it was due to intermolecular H-bonding between *β*-glucan and curcumin molecules (Figure 2.12) (Le et al., 2016).

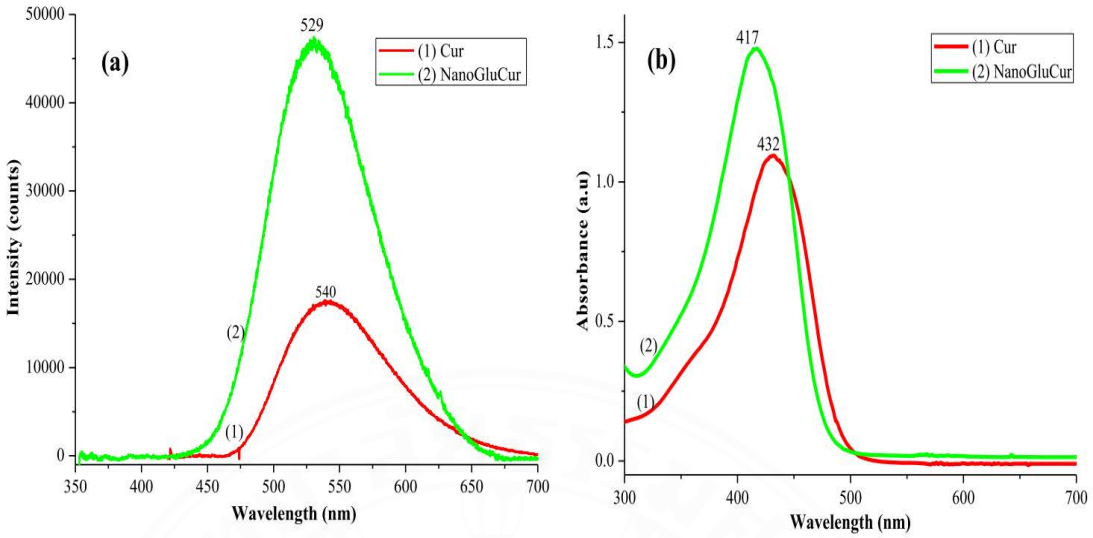

Figure 2.12 (a) Fluorescence intensity and (b) UV/Vis absorption of pure curcumin and curcumin-β-glucan combination (Le et al., 2016).

Verification of the fluorescence nature of pristine β-glucan, curcumin, and physical mixture before pH adjustment and after adjustment have also done by using the fluorescence microscope which measured excitation wavelength at 495 nm and emission wavelength at 530 nm. As shown in Figure 2.13 pristine yeast cells cannot attribute fluorescence brightness under given excitation wavelength. Curcumin has native fluorescence itself and even without yeast cells, it gives intense emission indication that curcumin was recrystallized during pH adjustment. When it combines with yeast cells under physical alkaline conditions, only the fluorescence crystal of curcumin was observed (Figure 2.13). suggesting that interaction require pH-shifting. Only yeast-shaped fluorescence emission was observed without curcumin crystals was seen outside revealing the successive binding.

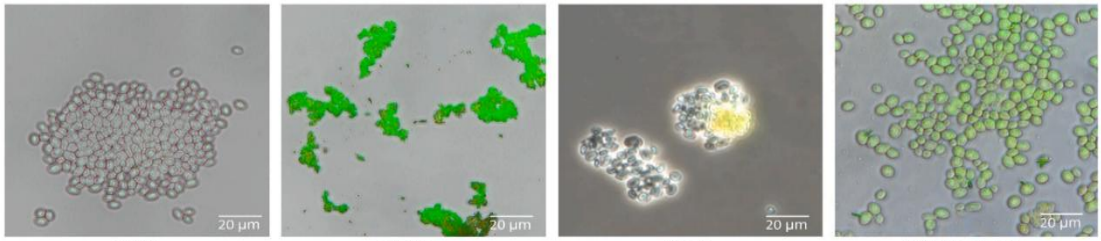

Figure 2.13 Fluorescence micrographs of YCs (yeast cells), CUR (curcumin), PM (physical mixture without pH adjustment), and CUR-YCs (after pH-driven adjustment) (Fu et al., 2022).

2.4.1 Possible factors affecting the binding of curcumin to *β*-glucan

2.4.1.1 pH Effect

Curcumin structure has heptadienone linkage connecting the two methyl phenyl function groups that possess the highly activated carbon atoms. Under the pH environments, multiple functional groups in curcumin can undergo protonation or deprotonation resulting in the alteration of the tautomeric structure of curcumin. In acidic and neutral conditions (pH 3 to 7), the keto form tends to predominate. C-H bonds associated with these carbon atoms are relatively weak due to the delocalization of electrons facilitated by adjacent oxygen atoms. Therefore, heptadione moiety performs as an electron donor which binds the electron-deficient species at pH 3 to 7. Conversely, the enolate form of the heptadienone chain takes over the responsibility as an electron donor and the underlying mechanism was more resemble that of the scavenging activity of phenolic antioxidants at pH levels exceeding 8 (Kumavat et al., 2013). According to these different mediums impact to curcumin structure, the absorption spectrum also exhibits variation. In the diketo form λ_{max} was observed at 360 nm while the keto−enol form was shifted to 428 nm (Figure 2.6) (Mabrouk et al., 2021). In acidic media, curcumin exhibits moderate solubility with a yellow color, while not fully dissolving in a neutral medium that produces a pale yellow color. Curcumin demonstrates high solubility under pH > 8 leading to the solution with dark orange color (Figure 2.14**)** (Wulandari, Sunarti, Fahma, & Enomae, 2020). Curcumin is not soluble in water, but its solubility can be enhanced by alkaline

conditions due to the ionization of phenolic groups. However, the curcumin structure was less stable in these alkaline circumstances (Chignell et al., 1994) and can break down to products such as vanillin, feruloyl methane, and ferulic acid (Boruah et al., 2012). Curcumin possesses two acidic hydrogens from phenolic and methylene groups of two diketones which have pKa values of 7.8, 8.5, and 9.0 respectively (Patra, & Barakat, 2011).

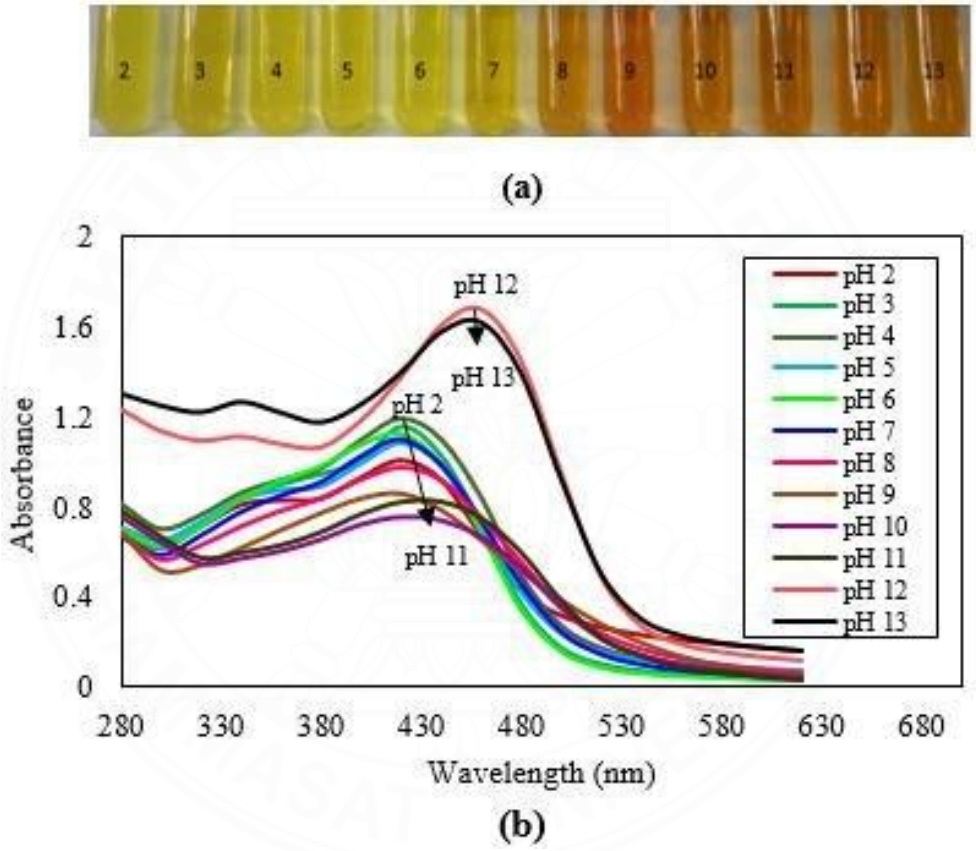

Figure 2.14 The curcumin color changes from pH 2-13 (a), and the curcumin UV-VIS spectra at pH 2- 13 in the range λ 280-620 nm (b) (Wulandari et al., 2020).

2.4.1.2 Ratio of fluorophore and *β*-glucan

Mass ratio of *β*-glucan and curcumin is also a critical factor for binding. When there are insufficient binding sites in *β*-glucan, it can lead to precipitation of curcumin consequently lowering the loading efficiency. Figure 2.15

indicated that when mass ratio was over 0.1, the precipitation of curcumin was observed in fluorescence micrographs.

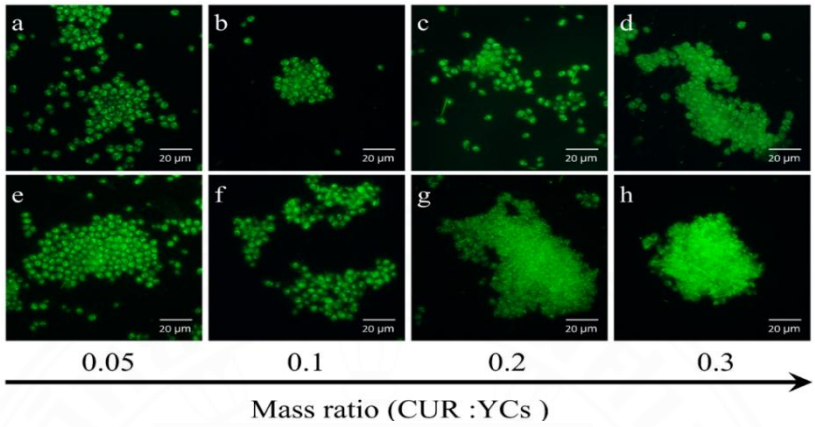

Figure 2.15 Fluorescence micrographs of a-d curcumin concentration (0.5, 1, 2 and 3 mg/mL) and e-h yeast *β*-glucan concentration (20, 10, 5 and 3.33 mg/mL) (Fu et al., 2022).

2.4.1.3 Effect of Salt

Salts (NaCl) stand out as an effective candidate for facilitating H-bonding and the presence of it can promote the intermolecular H-bonding and affect the excited state intramolecular proton transfer of curcumin. The addition of NaCl can increase the fluorescence intensity of the curcumin (Figure 2.16) (Ghatak, Rao, Mandal, Ghosh, & Sarkar, 2012). The electrostatic nature of salts also significantly influences the complexation of polysaccharides and proteins. Low salt concentration promotes the interactions by diminishing the electrostatic repulsion allowing more favorable molecular interactions. In contrast, high concentrations of salts reduce the net charge of biopolymers rendering the shielding for interaction. Due to its neutral ion properties, NaCl is often employed as a standard for assessing the ionic strength of the interaction. There are a number of studies that confirmed the enhancement of complexation of polysaccharides and proteins in the presence of NaCl. For instance, complexation of *β*-lactoglobulin and pectin, the optimized condition was achieved through in the presence of 0.21 M NaCl. When the binding of bovine serum albumin with k-carrageenan and ovalbumin with chitosan, NaCl also plays a critical role, and the optimized condition

for this interaction is typically reported to be 50 mM NaCl concentration (Zhong et al., 2022). Therefore, the study of the NaCl effect should be involved when investigating the binding of curcumin and β-glucan molecules.

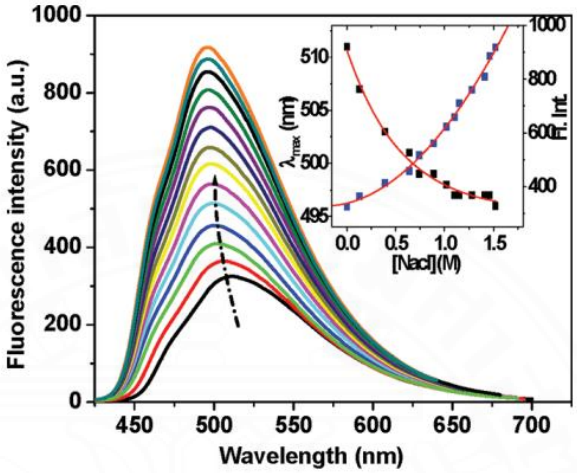

Figure 2.16 The fluorescence intensity of curcumin in the presence of NaCl is up to 60 mM (Ghatak et al., 2012).

2.4.1.4 Temperature Effect

The temperature-dependent optical properties of curcumin by using in situ temperature-dependent UV/Vis absorption spectroscopy from 20°C to 95°C was studied and three peaks were observed at 237, 345, and 419 and became prominent as the temperature increases. Thermal energy can break the intramolecular H-bonds of keto-enol functional groups in curcumin which are responsible for interacting with polar functional groups in solvent. Therefore, the intensity of curcumin is considerably changed in water when increased in temperature. In general, π–π* and the n–π* transitions can render the solvochromic shifting towards longer wavelength (red-shifted) or shorter wavelength (blue-shifted) depending on the polarity of the solute and solvent. In this study, they found that the curcumin in water occurred to blue shift when increased in temperature (Figure 2.17a). The behavior of the blue shift can be due to two factors (1) high thermal energy obstructs the intermolecular H-bonding and increases transition energy and or (2) the cyclic structure within curcumin displays a decrease in conjugation effect. Dipolar interactions and H-bonding are pivotal factors

that determine the molecular absorption and fluorescence properties of the compounds. As the temperature increases, its high energy can break down the intramolecular H-bonding of the curcumin functional groups and can enhance the interaction with water molecules. These environmental changes can affect the energy transition of the molecules that intend to alter the absorption and optical properties. However, the optical properties of curcumin were less affected by dissolving in the organic solvent (Figure 2.17b) (Jagannathan, Abraham, & Poddar, 2012).

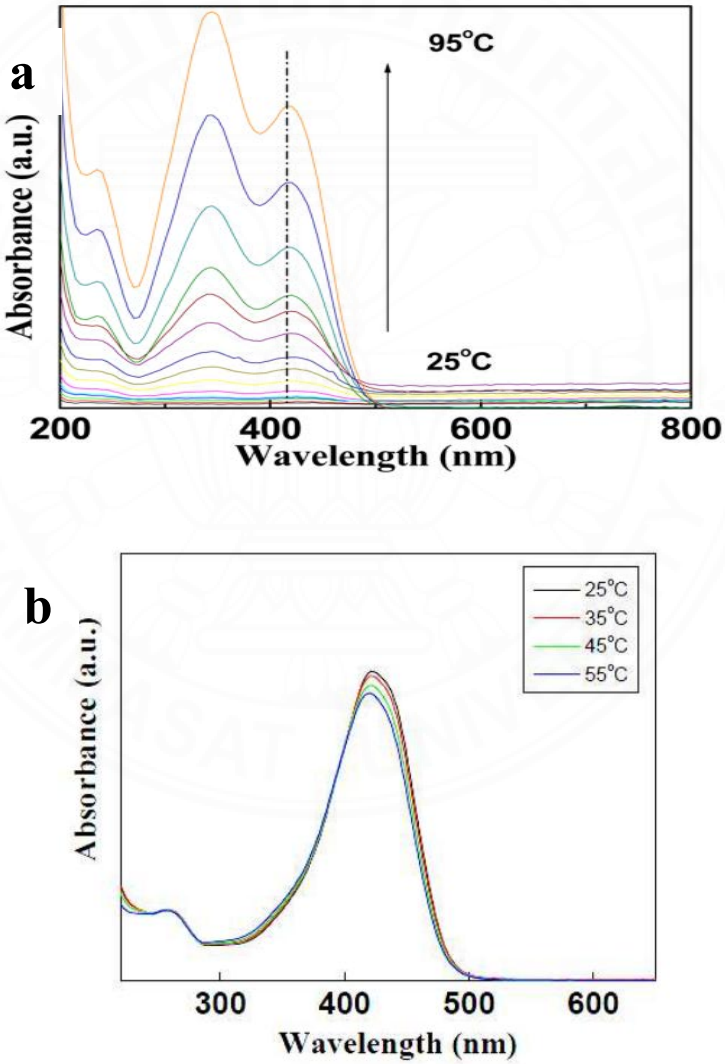

Figure 2.17 Temperature effect of curcumin's absorption in a) water and b) methanol (Jagannathan et al., 2012).

2.4.1.5 Excitation and Emission wavelength

Curcumin is a hydrophobic compound and does not well dissolve in water but is readily dissolved in ethanol. The yellow color of the curcumin in ethanol solution absorbs UV light at approximately 420 nm. It can also exhibit characteristic fluorescence emission which will be centered at 525 nm. However, its fluorescence optical properties is excitation wavelength dependent and can vary upon certain excitation (Figure 2.18a) (Guo, Yang, Zhang, & Tao, 2022).The interaction between curcumin and its surrounding solvent can also influence the excitation and emission wavelength maxima (Figure 2.18b). (Erez,Simkovitch, Shomer, Gepshtein, & Huppert, 2014).

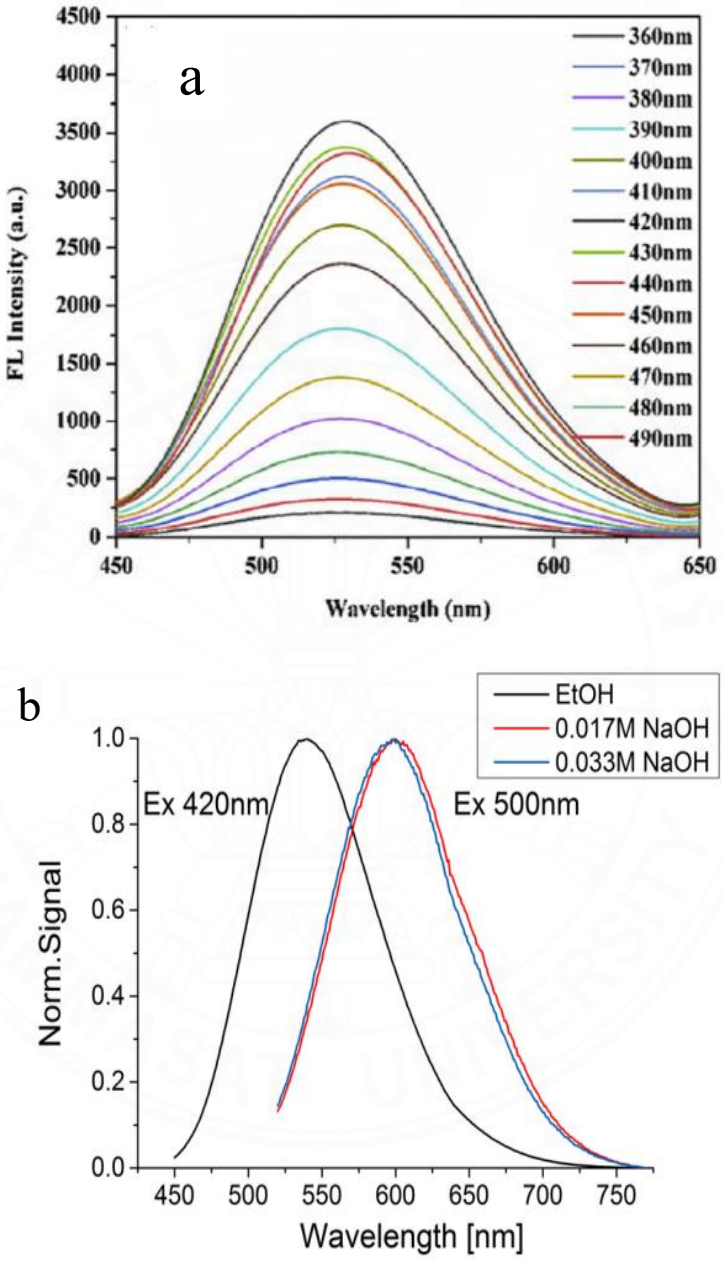

Figure 2.18 a) Curcumin's excitation wavelength maxima vary on different excitation wavelengths. b) Different emission and excitation wavelengths for different solvents (Guo et al., 2022; Erez et al., 2014).

2.4.1.6 Stability

Yellow color is an indicator of curcumin degradation and its stability. Therefore, a UV/Vis spectrophotometer was used to monitor the changes in color intensity over time. The absorption intensity was reduced in all pH as time progressed, but the rate of degradation depends on the pH of the solution. The decrease in absorbance of the curcumin was slower in acidic conditions than in alkaline solution. Under neutral conditions, the absorbance was notably decreased within 7min with the degradation rate value of 92, 135, and 125 cm^{-1}/min for pH 7, 7.4, and 8 respectively (Figure 2.19) (Kharat et al., 2017). The conjugated diene structure in curcumin was believed to be responsible for stabilizing under acidic conditions. When pH was adjusted to neutral or basic condition, the proton was removed, and this structure was destroyed. After 60 min experiments, the amount of curcumin remained in the order of pH 1.2 > pH 1 > distilled water > pH 6.8 > pH 7 > pH 7.4 (Kumavat et al., 2013) The decrease in absorbance occurs more rapidly under acidic conditions when stirring (Figure 2.20). This was suggested that stirring facilitates the nucleation and crystallization of curcumin in aqueous medium leading to a decrease in absorbance. Therefore, continuous stirring should be avoided during the experiments. As described above the keto-enol tautomer of curcumin structure stability also greatly depends on temperature changes. Therefore, temperature and pH are the considerate factor for reaction response and stability of the experiments.

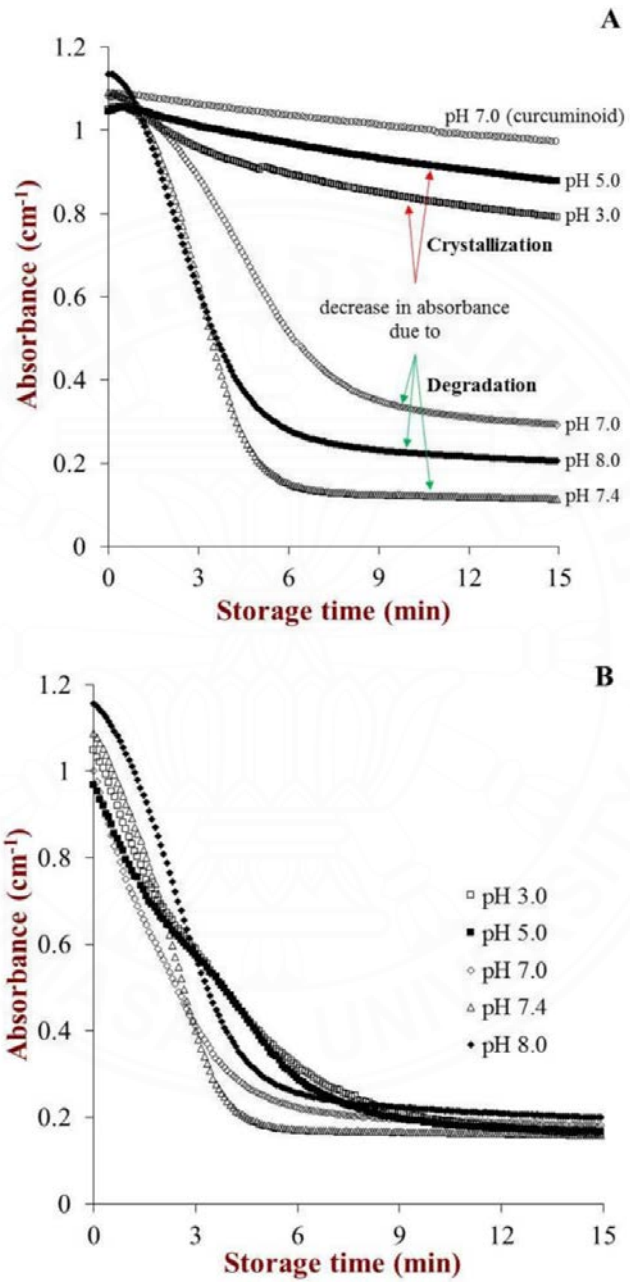

Figure 2.19 Stability of curcumin (40 μM) in phosphate buffer solutions (10 mM) of various pH values when the system was unmixed (A) and mixed (B) (Kharat et al., 2017).

CHAPTER 3
RESEARCH METHODOLOGY

3.1 Materials

Lentinus squarrosulus (Herd Khon Khao) mushrooms were purchased from Thailand's local market, freeze-dried, and ground to get the fine powders. *Lentinula edodes* (Shiitake) mushroom powders were purchased from Myskin recipes. Curcumin (C1386) was purchased from Italmar Co., Ltd. Curdlan Standard (C7821) was purchased from Colossal International Co., Ltd. Ethanol used was 99% analytical grade. Aniline blue (C.I. 42755) UK Germany was purchased from Colossal International Co.,ltd. Fluorescence brightener 28 (Calcofluor white) was used for Calcofluor fluorescence analysis. (Citric acid (MW-210) and sodium hydroxide (MW-40) were analytical grades. All the reagents and stock solutions were prepared with distilled water.

FP-6200 Spectrofluorometer (Jasco Co., Ltd) was used for fluorescence measuring. A domestic microwave system (EMM2023MW-20L) from Electrolux Co., Ltd with 700 watts was used for microwave extraction. iS50 FRIT instrument from Thermofisher Scientific was used for FTIR measurement.

3.2 Methods

3.2.1 Extraction of *β*-glucan

3.2.1.1 Alkaline and Hot Water Extraction

Fresh bodies of *Lentinus squarrosulus* mushrooms purchased from the local fresh market were cleaned thoroughly and cut into small pieces. The extraction procedure followed the previously studied method with some modifications (Shaheen et al. 2022). Fresh fruit bodies of mushrooms were freeze-dried overnight and ground into powder to get a dry weight of approximately 6%. 20 g of dried mushroom powdered was firstly subjected to hot water (1:10 ratio) at the temperature of 90-100°C for 14 hours with a Soxhlet extractor. The water extract was precipitated with three times the volume of ethanol and kept overnight. The precipitate was then collected by

centrifugation at 8000 rpm for 20 min followed by dialyzing against distilled water (Membrane M.W CO – 12000 to 14000) for 7 days and freeze-dried which was regarded as hot water extract (HWE). The residues were subsequently treated with methanol at a temperature of 60-80°C for 8 hrs. to remove the excess protein residues in the sample. Finally, the residues were treated with 1 M NaOH solution for 12 hrs. with Soxhlet apparatus. The soluble fractions were neutralized with 0.4 N HCl and precipitated with three times the volume of ethanol. Final precipitates were washed with distilled water and ethanol (1:3) and collected by centrifuging at 8000 rpm for 20 min. The precipitates were dialyzed against distilled water (Membrane M.W CO – 12000 to 14000) for 7 days and freeze-dried. The dry sample for alkaline extraction was denoted as AE and prepared for further analysis.

3.2.1.2 Microwave Extraction

A domestic microwave system (EMM2023MW-20L) from Electrolux Co., Ltd with 700 watts was used for this purpose. Since the (1:10) ratio did not provide sufficient water for the dissolution of mushroom powder, the (1:20) ratio was used instead for this purpose. 2 g of dried mushroom was subjected to 40 ml of distilled water and heated in a microwave at medium heat for 60 sec. The time is limited to 60 sec because exceeding this time may result in solvent overflowing from the container. The resulting supernatant was precipitated with three times the volume of analytical-grade ethanol and left overnight. The residues were collected, dialyzed, and freeze-dried as described above. The microwave extracts were labeled as ME.

3.2.2 Solution Preparation

Curcumin stock solution was prepared by dissolving 10 mg of curcumin in 10 ml of ethanol (1000 ppm). Further dilution can be followed with distilled water and it is crucial to prepare the dilution just before analysis since the degradation of curcumin was faster in an aqueous solution.

Aniline blue stock solution was prepared according to the previous study (Koenig, Rühmann, Sieber, & Schmid, 2017). 12.7 ml ultra-pure water, 3.70 ml glycine/NaOH buffer (1.0 M glycine, 1.25 M NaOH), 1.31 ml 2 M HCl, and 2.50 ml dye solution (5.0 g/l Aniline blue) were mixed and stored in a dark environment overnight to decolorize and stable.

Calcofluor fluorescence brightener was prepared by directly adding 20 µL into 100 ml of 0.1 M of $NaHCO_3/Na_2CO_3$ buffer, pH 10.

The standard curdlan was prepared by dissolving 10mg in 0.01 M of NaOH to get a 1000ppm stock solution. All the samples to be examined were also dissolved in 0.01 M of NaOH solution.

3.2.3 Curcumin Fluorescence Assay (Proposed Method)

The standard *β*-glucan or sample solution was mixed with curcumin under alkaline conditions at pH 11. The solution subsequently changed the pH by adding citric acid. The mixture was vortexed for 20 sec to ensure homogenization. The fluorescence intensity was measured at the excitation wavelength of 420 nm and the emission wavelength was scanned from 430 to 700 nm. The conditions for the method including pH adjustments, curcumin concentrations, and other factors were applied according to the optimization.

3.2.4 Aniline Blue Fluorescence Assay

A sample or standard solution of *β*-glucan was mixed with a 1:1 ratio of Aniline blue solution that was prepared in section 3.2.2. The fluorescence emission of the complex was scanned from the range of 415 to 700 nm by excitation at 405 nm. Curdlan was a standard to draw the calibration curve in the linear range of 2-20 ppm.

3.2.5 Calcofluor Fluorescence Assay

A sample or standard solution of *β*-glucan was mixed with a 1:1 ratio of prepared Calcofluor solution in section 3.2.2. All prepared solutions were carefully placed in dark environments because Calcofluor was extremely light-sensitive and affected the intensity. The fluorescence intensities were measured by excitation at 380 nm and emission wavelength was scanned from 390 nm to 600 nm. Curdlan was used as the standard to draw the calibration curve in the range of 2 – 20 ppm.

3.2.6 Interaction study of curcumin and *β*-glucan with FTIR

To investigate the interaction between curcumin and *β*-glucan, a Fourier Transform Infrared Spectrometer – Attenuated Total Reflectance (FTIR-ATR) was employed. The preparation of the solution followed the pH-driven method as in the reference with some modifications (Fu et al., 2022). The curcumin 4 ppm was mixed with 10 ppm curdlan standard solution in alkaline media and the solution pH was immediately adjusted back to acidic pH 3. The solution was then centrifuged at 15000

rpm for 10 minutes at 4°C (Supra R30 centrifuge from Hanil Co.,Ltd). The precipitates were then freeze-dried to test FTIR. The highly sensitive FTIR-ATR technique was used to detect the corresponding stretching vibration behavior of two molecules after mixing.

3.2.7 Optimization of Experimental Parameters

All the optimization experiments were conducted by using 10 ppm *β*-glucan standard solution and 4 ppm curcumin solution. Firstly, 10 ppm of the *β*-glucan standard solution was mixed with 4 ppm of curcumin solution under an alkaline pH of 11 which was greater than the pKa value of enolic and phenolic functional groups of curcumin (pKa; 7.8, 8.5, and 9.0). Subsequently, the pH was adjusted back to optimal pH value and the solution was vortexed for 20 sec. The resulting solution was analyzed by fluorescence spectrophotometer.

3.2.7.1 Optimization of Excitation and Emission Wavelength

To determine the optimal excitation and emission wavelength that offers the intense and stable fluorescence emission maxima, the stoke shift between excitation and emission was evaluated. The emission wavelength was initially set to 550 nm and 540 nm based on the previously reported value (Jagannathan et al., 2012). The excitation wavelength was scanned from 300 nm to 500 nm. Using the resulting excitation wavelength the emission maxima were optimized. The stoke shift within the excitation and emission maxima was calculated as $\Delta\lambda = \lambda_{max}^{ex} - \lambda_{max}^{em}$ (Valeur & Berberan-Santos, 2012).

3.2.7.2 Optimization of pH

Since the interaction was driven by pH adjustment, pH was the critical parameter in this study. The procedure follows the same as in section 3.2.7. After the deprotonation step, the ideal pH ranging from 2 to 7 was adjusted for efficient binding of curcumin and *β*-glucan. Following the vortexing for 20 sec, the stability of the intensities was monitored with optimal excitation and emission wavelength of the previous study.

3.2.7.3 Optimization of the Effect of Salt

The impact of salt was determined whether it can enhance the rate of reaction, stability, and solubility of the reaction. The common salt NaCl was chosen, and the concentration range (5, 10, 15, 20, 30, 50, 100, 150, 200 mM) was

added to the β-glucan standard solution prior to mixing with the curcumin compound. Subsequently, the solution was adjusted back to the optimal pH, vortex for 20 sec, and conducted the fluorescence test.

3.2.7.4 Optimization of the ratio of fluorophore

To optimize the ratio of fluorophore and analyte for maximizing the fluorescence signal, various curcumin concentrations (1 to 20 ppm) were mixed with different levels of β-glucan concentration (1,2,5,10,15,20 ppm) for lower limit and (20,30,40,50 ppm) for higher limit. Using the resulting data, draw a calibration curve to achieve the linear response of the analyte with specific fluorophore concentration. The experiments follow the same procedure as in section 3.2.7.

3.2.7.5 Optimization of Temperature

Considering that the equilibrium of tautomerism within curcumin structure can be influenced by the temperature treatment, the temperatures 40°C and 60°C were investigated and compared with room temperature value. The procedure was followed as in section 3.2.7. After the deprotonation step and pH adjustment, the solution was incubated in the water bath at constant temperature (40°C ± 1°C and 60°C ± 1°C) for 20 min. After heat treatment, the solution was cool down to room temperature for 5 min and the fluorescence intensities were measured. 10 replicates experiments were performed to investigate the robustness and stability of the temperature treatment.

3.2.8 Stability Study

Three aspects of stability studies was assessed including monitoring the reaction stability study, Reagent shelf-life under specified storage conditions, and the sensitivity of light. After optimizing the ideal conditions, the fluorescence intensities were recorded continuously for 1 hour to ensure the stability of the reaction.

To know the shelf-life of the reagent the curcumin stock solution dissolved in the ethanol and β-glucan standard solution (1000 ppm) were stored in °C under daylight. The curcumin stock solution was diluted with distilled water to the desired concentration and β-glucan was diluted to 10 ppm just prior to the analysis and measured the fluorescence intensities for five consecutive days.

Since curcumin might be sensitive to light the measurement was conducted under environmental light for 30 min and compared with other fluorophores (Aniline blue and Calcofluor).

3.2.9 Analytical Method Validation

Analytical method validation was performed in compliance with the ICH (International Council for Harmonization) guideline. The linear range was evaluated by selecting the β-glucan concentration range from 1 to 60 ppm using the optimized amount of curcumin concentration. The curdlan was used as a calibration standard and calculated the linear regression through the calibration curve. The limit of detection (LOD) and limit of quantification (LOQ) were verified by analyzing 10 replicates of the blank solution (curcumin only) and calculated as follows.

$$\text{LOD} = 3.3\ \sigma / S; \quad \text{LOQ} = 10\sigma / S$$

σ is the standard deviation of the 10 replicates of the blank solution and S is the slope of the calibration curve.

The precision of an analytical procedure was studied by integrating the area of the β-glucan standard solution of (20,40,60 ppm) for curcumin level 10 ppm concentration and (10, 15, 20 ppm) for 4 ppm curcumin concentration, and % relative standard deviation was calculated.

The accuracy of the proposed method was determined by spiking a known amount (10 ppm) of standard in each sample. The percentage recovery and the level of spiking were calculated as follows.

$$\text{Recovery (\%)} = \frac{\text{Cspike sample} - Csample}{\text{Cstandard}} * 100$$

3.2.9 Statistical Analysis

All analyses were performed in triplicate and the results were reported as mean ± standard deviation. Comparisons of different groups were conducted by using

one-way ANOVA for variance of the samples, with the P-values < 0.05 assumed statistically significant.

CHAPTER 4
RESULTS AND DISCUSSION

4.1 Interaction study of curcumin and *β*-glucan with FTIR

Previous studies have stated that the interaction between curcumin and *β*-glucan primarily involves hydrogen bonding and hydrophobic interaction. Therefore, this interaction was elucidated with the employment of FTIR spectra. The characteristics of stretching vibration spectra of native curcumin and curdlan (*β*-glucan standard) were illustrated and compared with the mixture of curcumin and curdlan using the pH-driven method. The spectra were interpreted by the previous findings (Fu et al., 2022; Le et al., 2016). The major O-H stretching of the phenolic group in native curcumin was found at 3502 cm^{-1}. The stretch vibration at 1627 and 1600 cm^{-1} was attributed to the (C=O) bond vibration and structural integrity of the benzene ring. The band at 1504 cm^{-1} and 1427 cm^{-1} corresponded to the mixed vibration of (C=O; C=C) of the aromatic ring and alkenyl H-bond stretching of curcumin respectively. The remaining 1267 cm^{-1}, 1024 cm^{-1}, and 959 cm^{-1} represent the aromatic C-O stretching, methoxy C-O-stretching, and aromatic C-H stretching (Figure 4.1). The characteristics of *β*-configuration of the polysaccharide were also clarified in Figure 4.1 by the bands at 3311 cm^{-1} for O-H stretching and 888 cm^{-1} for the anomeric region of *β*-glucan. Another prominent spectrum at 1160 and 1031 cm^{-1} indicated the presence of the structural backbone of glucose polymer. After interaction through the pH-driven method, the O-H stretching band of curcumin at 3502 cm^{-1} merged with the band of *β*-glucan meaning that these two compounds interact across hydrogen bonding. Additionally, the structural backbone vibration of the aromatic ring and C=O bands of curcumin at 1627, 1600, and 1504 cm^{-1} faded within the spectra of the complex due to the masking of molecular vibration of *β*-glucan at the range between 1700 to 1500 cm^{-1} (Mohan, Sreelakshmi, Muraleedharan, & Joseph, 2012). The characteristic vibration for aromatic C-H stretching of the curcumin band at 959 was not shown after loading (Peng et al., 2018). This indicated that curcumin was driven to the *β*-glucan core via hydrophobic force (Fu et al., 2022). Due to the interaction of curcumin with the

hydroxyl group of β-glucan, the band's region and 1160 cm^{-1} and 1031 cm^{-1} shifted to 1134 and 1029 cm^{-1}. Additionally, a slight shift of the anomeric region of β-glucan from 888 to 881 cm^{-1} was observed. The shifting was listed in Table 4.1. According to the finding the encapsulation was confirmed and the result aligned with the previous studies (Fu et al., 2022; Le et al., 2016).

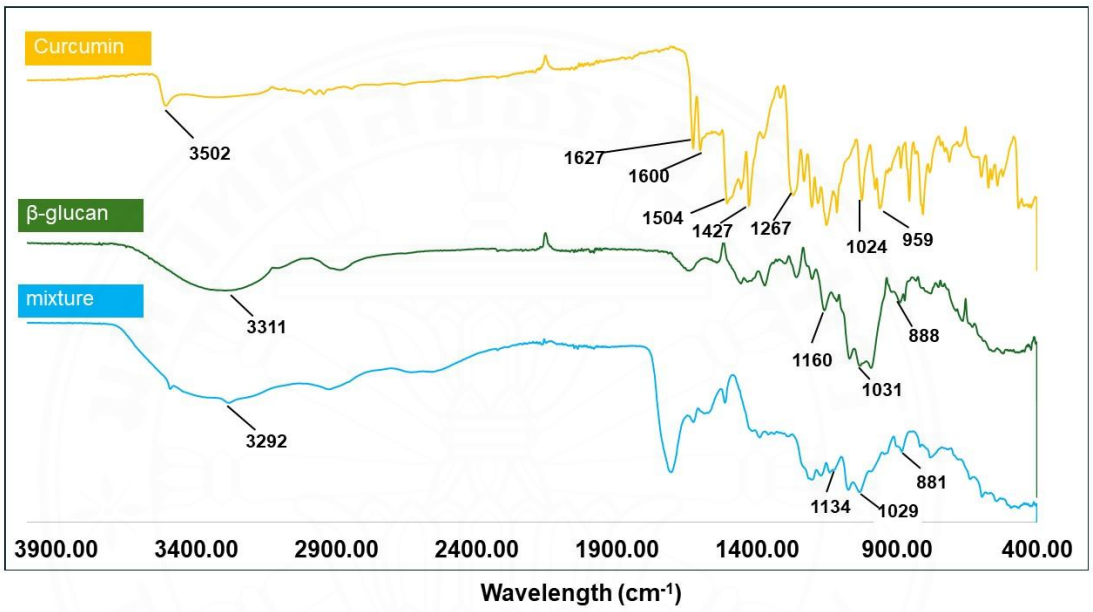

Figure 4.1 FTIR spectra of curcumin standard (Yellow), β-glucan standard (Green), and a freeze-dried sample of a mixture of curcumin (4 ppm) and β-glucan (10 ppm) by the pH-driven method (Blue).

Table 4.1 Characteristic spectra of curcumin, *β*-glucan, and their complex by pH-driven method and wavelength shifting presented after loading.

Wavelength (cm^{-1})		
Curcumin	*β*-glucan	Complex of curcumin & *β*-glucan
3502 (O-H)	3311 (O-H)	3292
1627 (C=O)		
1504 (C=C)		
959 (C-H) aromatic ring		
	1031-1160 (C-OH) (Polysaccharide backbone)	1029-1134
	888	881

4.2 Optimization Parameters

4.2.1 Optimization of Excitation and Emission Wavelength

It had been proposed that the absorption and emission spectra of curcumin greatly depended on the environmental condition (Bhatia et al., 2016). Generally, curcumin can present absorption peaks ranging from 300 to 500 nm. The fluorescence nature of the curcumin after binding with the *β*-glucan has been demonstrated to be a prominent enhancement and shifting to the higher wavelength energy due to the intermolecular hydrogen bonding between them (Le et al., 2016). Therefore, the initial emission wavelength was set at 540nm and 550 nm according to the previous values by Jagannathan et al. (2012) and the excitation wavelength was scanned from 300 nm to 500 nm. It was shown that the absorption maxima was observed at 420nm (Figure 4.2). Using this absorption value of 420 nm ± 10 nm the emission wavelength was optimized again. The larger stoke shift ($\Delta \lambda$ – 120 nm) and the higher intensities were achieved with 420 nm excitation wavelength and 540 nm emission wavelength which complied with the previous result (Jagannathan et al., 2012) (Figure 4.3) The stoke < 70 nm can lead to the self-absorption of emitted photons

and occurred unwanted background interferences (Gao, Hao, Zheng, & Chen, 2017). Therefore, 420 nm was selected for further analysis with subsequent emission scanning across 430 nm to 750 nm.

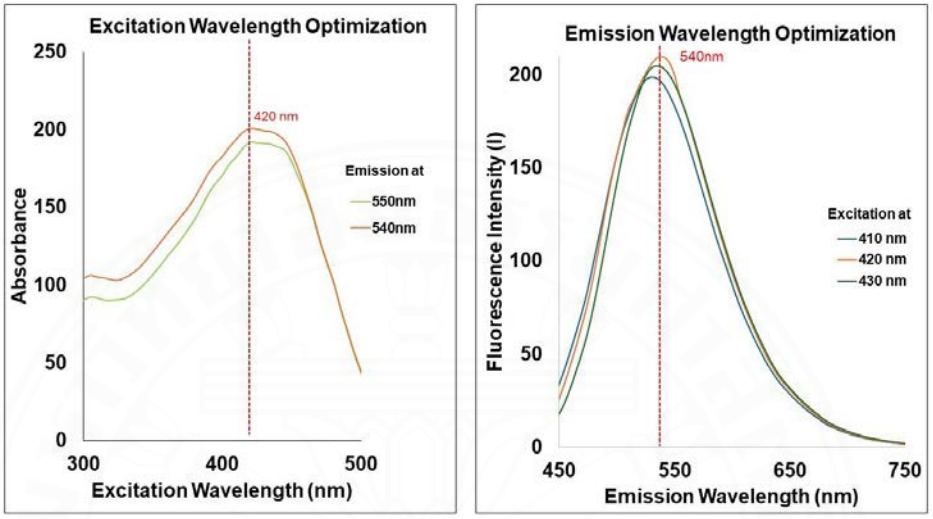

Figure 4.2 Optimization of the wavelength maxima (n=1).

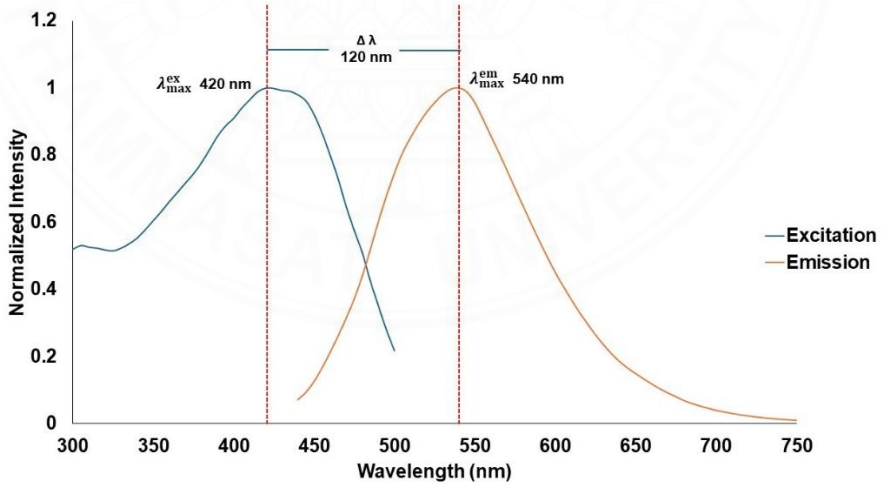

Figure 4.3 The wavelength maxima of absorption spectra and emission spectra at 420 nm and 540 nm respectively. Curcumin concentration (4 ppm) and β-glucan concentration (10 ppm) were used. The spectra were normalized to a peak maximum of 1 (n=1).

4.2.2 Optimization of pH

In this study loading of curcumin to β-glucan was done by pH-driven method in which method pH shifting facilitates the loading capacity of these two compounds (Fu et al., 2022). According to previous studies, both compounds first dissolved in pH 11 which is greater than the pKa of the protons of curcumin. The solution pH was then subsequently changed back to a lower pH level to form the hydrophobic force. The optimization range was set between 2 to 7 because over pH 7, the deprotonation stage occurred again and the intensities obviously reduce as seen in (Figure 4.4). The fluorescence intensities of the curcumin and β-glucan were also slightly reduced when gradually increasing the pH from 2 to 7. The stable intensities can be reserved within pH 2 to 4 with a 95% confidence level (P value < 0.05). Increasing basicity, curcumin can be deprotonated and lose its proton from the hydroxyl unit. During the first step in the pH-driven method, the high alkaline condition was treated to curcumin to be deprotonated to its amorphous nature. After the particular pH was adjusted back, its amorphous nature still intact and enhancing the binding with other compounds through hydrophobic and hydrogen bond interaction (Li et al., 2024). The finding is consistent with the previous research (Tang, Ma, Wang, & Zhang, 2002) that indicated the steady and strong absorption of curcumin can be maintained at pH 1.9 to 3.1. Consequently, the midpoint pH 3 was chosen to evaluate the method to withstand the fluctuation.

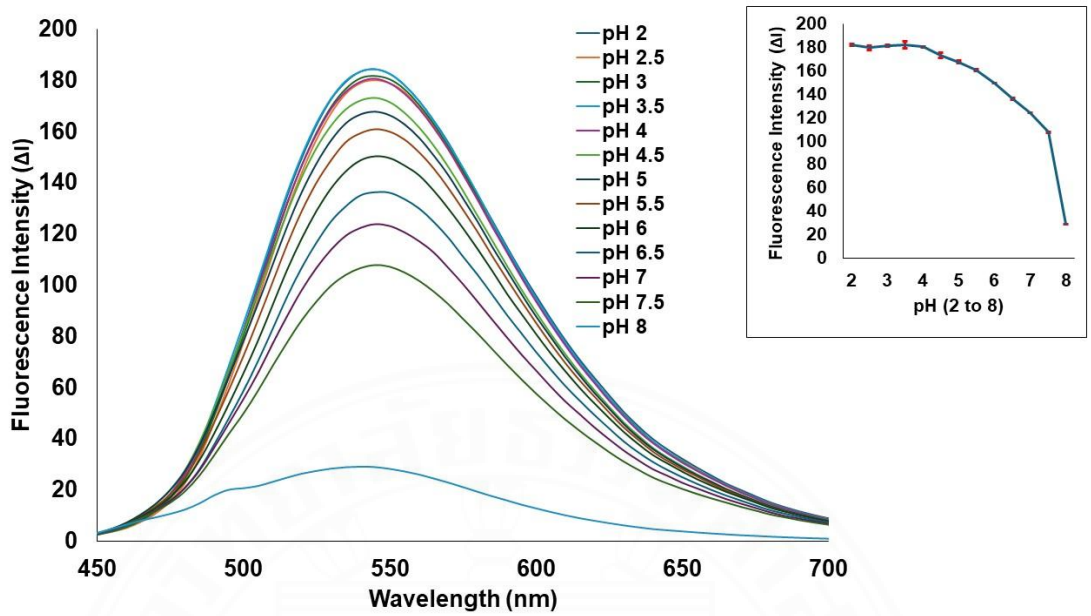

Figure 4.4 Fluorescence spectra of curcumin with different pH (2 to 8) in the present of *β*-glucan (n=3).

4.2.3 Optimization of the Effect of Salt

Ionic strength also influences the surface charge density of the molecular interaction that in turn affects the electrostatic force between them. The addition of salt may change the electrostatic force and hydrophobic interaction between the molecules. The impact of ionic strength on the stability of the curcumin molecules has been investigated by adding the NaCl concentration (5, 10, 15, 20, 30, 50, 100, 150, 200 mM). The result showed a slight decrease in the intensity of ± 0.01 when NaCl concentration exceeded 15 mM, compared to the intensity without adding salt. Notably, a decline was observed at higher NaCl concentrations of 150mM and 200mM (Figure 4.5). The steady-state fluorescence intensity of the mixture can be reserved at the NaCl concentration of up to 15 mM (P value >0.05). It can be implied that the ionic strength might affect the stability of the interaction because the hydrolytic degradation of curcumin in its neutral form can be accelerated by catalyzing with Cl^- ion present in salt. However, the method remains robust within the ionic strength of 0.01 M (NaCl 15 mM) thresholds.

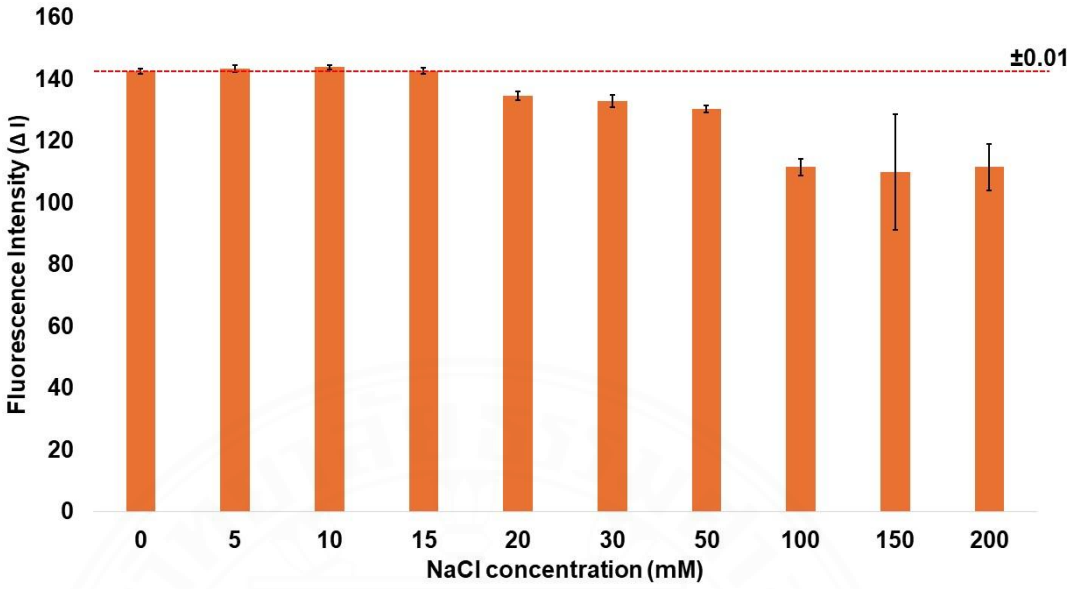

Figure 4.5 The stability of the fluorescence intensity in different ionic strengths (5, 10, 15, 20, 30, 50, 100, 150, 200 mM); n=5.

4.2.4 Optimization of the ratio of fluorophore

The present study deals with the development of the fluorescence intensity when curcumin complex with the *β*-glucan molecules. The concentration of curcumin molecules plays an essential role in evaluating whether to provide enough binding sites for the *β*-glucan molecules because the excess curcumin molecules can render precipitation (Fu et al., 2022). In this study curcumin concentration from 1 to 20 ppm was tested to investigate the limited binding site of curcumin with the *β*-glucan molecules. It was found that over 10 ppm curcumin concentration, the fluorescence intensity started to reduce, and a poor signal-to-noise ratio was observed (Figure 4.6). From the range of 1 to 10 ppm curcumin molecules, it was shown that 4 ppm curcumin concentration can give the stable and linear combination for the lower concentration of *β*-glucan compound up to 10ppm, while 10 ppm curcumin concentration can give stable binding sites for higher concentrations of *β*-glucan up to 60 ppm with the linear regression value of 0.99 respectively (Figure 4.7 & 4.8). It means a higher concentration of *β*-glucan may not effectively bind to a certain amount of curcumin and become saturated making to bend the calibration curve. Therefore, in our study 4 ppm curcumin

concentration was used for lower β-glucan concentration and 10 ppm curcumin concentration for higher levels to study the linear response.

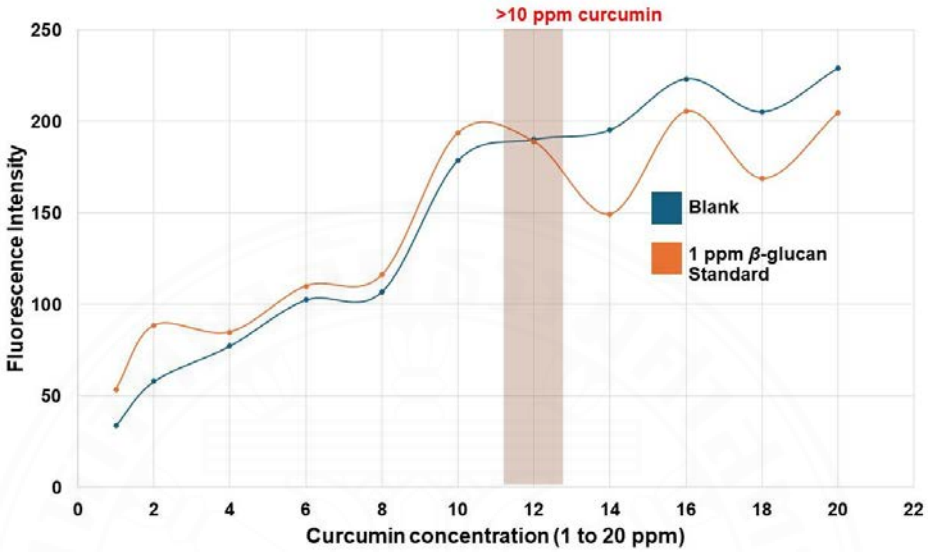

Figure 4.6 Fluorescence signal of curcumin only solution (blue) and binding of curcumin and 1 ppm β-glucan standard solution by increasing the curcumin concentration from 1 to 20 ppm n=1.

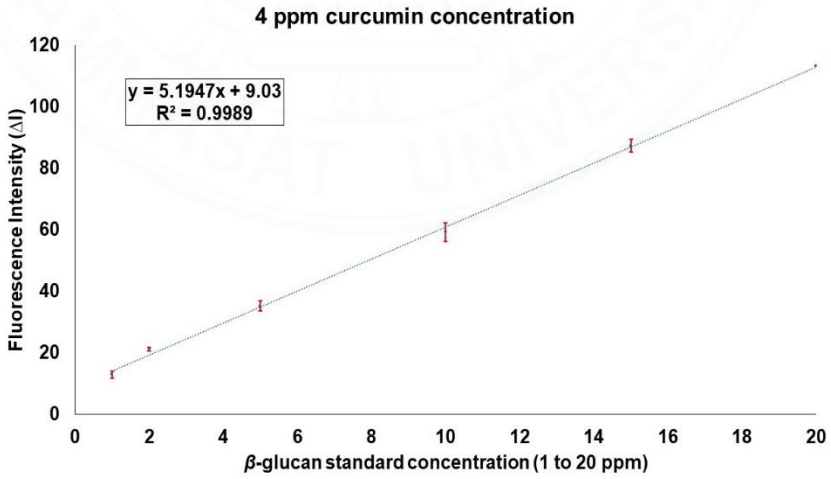

Figure 4.7 Linear Response of β-glucan concentration from 1 to 20 ppm loaded with 4 ppm curcumin concentration: n=3.

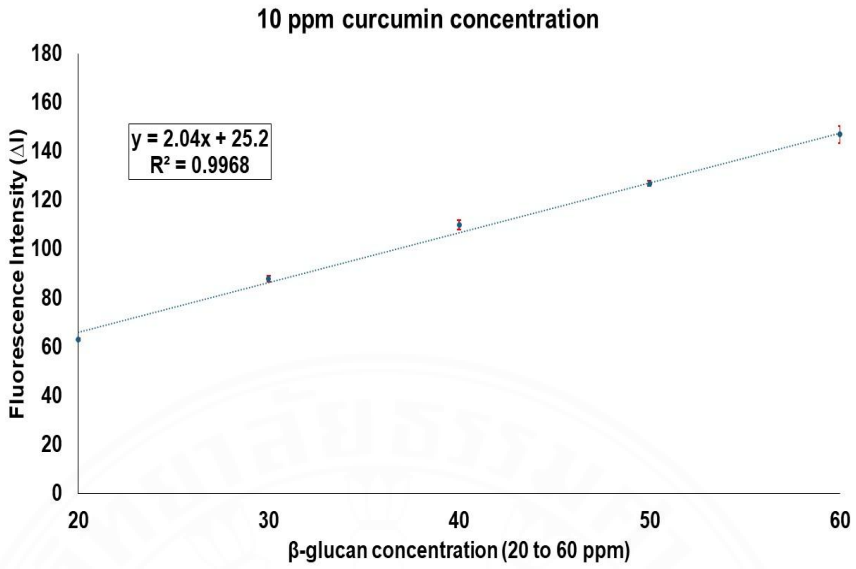

Figure 4.8 Linear Response of *β*-glucan concentration from 20 to 600 ppm loaded with 10 ppm curcumin concentration: n=3.

4.2.5 Optimization of Temperature

Curcumin possesses the keto-enol tautomeric functional groups in its main structure. The different tautomeric arrangement defines the strength and nature of binding with other biological molecules. Temperature significantly impacts the equilibrium of tautomeric conformation leading to shifting the ratio of equilibrium (Bhatia et al., 2016). In this study, three temperatures; ambient temperature, 40°C, and 60°C was investigated for 20 min. Room temperature exhibited little variation in the first 5 min and becomes stable until 20 minutes. For 40°C and 60°C, the intensity starts to stabilize at 6 and 7 min (Figure 4.9). Although the stability can build up within 7min, with the treatment of temperature (40 and 60°C) there can be impairment in binding with *β*-glucan. The performance presents poor robustness after thermal treatment in (Figure 4.10). When the temperature is increased the reactive enol form shifts to the diketo form which has a lesser binding affinity. Thermal energy can break the intramolecular hydrogen bond of enol conformation resulting in the increasing of diketo moiety. But this phenomenon is reversible and after cooling the form can shift back to its original state (Bhatia et al., 2016). It was proposed that the tautomeric resonance

stability can be significantly impacted by increasing temperature (Jagannathan et al., 2012). It can be concluded that the shifting of this equilibrium during the heating and cooling cycle cannot control the steady state of binding interaction with β-glucan and can cause inadequate robustness. Hence, room temperature incubation will carried out for further study. A summary of the optimization parameters were described in Table 4.2.

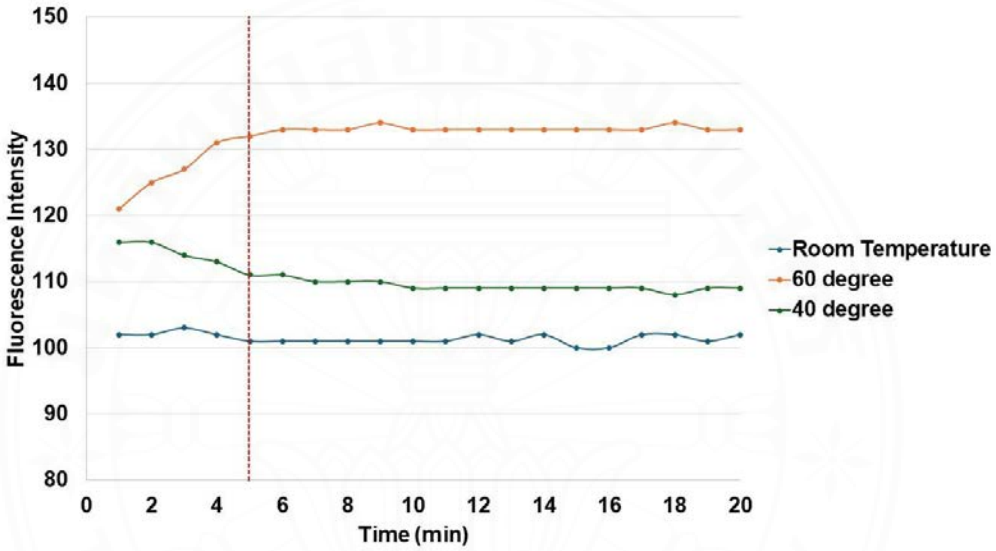

Figure 4.9 Stability Testing of curcumin and β-glucan after temperature treatment (n=1).

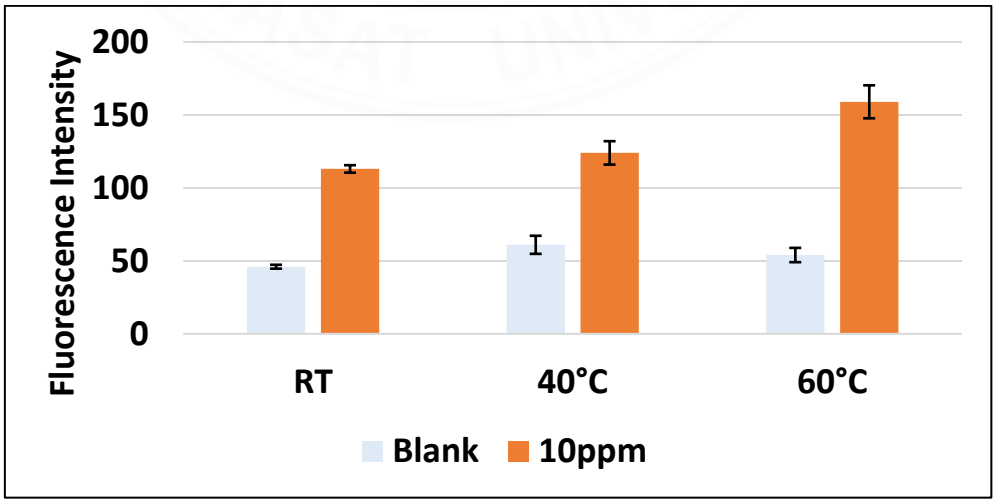

Figure 4.10 The poor robustness in increasing temperature (n=10).

Table 4.2 Summary of Optimization Parameters.

Optimization Parameters	Achieved Values
Excitation & Emission Wavelength	420 nm & 540 nm
Adjustable pH after deprotonation	pH 3
Effect of Salt	decrease intensity if > 15mM of NaCl
Ratio of fluorophore	4 ppm curcumin for (1 to 20 ppm *β-glucan* range) 10 ppm curcumin for (20 to 60 ppm *β-glucan* range)
Temperature	Room temperature

4.3 Stability Study

While developing the quantitative measurement with fluorescence intensity, the stability of the fluorophore is a greater concern to regulate the signal-to-noise ratio with constant results in order to obtain reliable data. After getting the optimization condition with stable conditions, the fluorescence intensities for the binding mixture was monitored. The stable intensity was achieved within 1 hour period (P value < 0.05) for both curcumin only blank solution and mixture with standard solution (Figure 4.11). The results indicated that the optimized parameters were effective for the stable measurement of *β*-glucan with the curcumin fluorophore. The storage stability of the reagent stock solution was examined the intensity slightly reduced after two days and it is more pronounced by day 3 as illustrated in Figure 4.12.

Light-induced structural alteration of fluorophores can indeed be a challenge for the development of analytical methods. For instance, light exposure allows the transition of Calcofluor trans to cis form which is unfavorable to bind with *β*-glucan (Wu et al., 2008). In Figure 4.13, curcumin exhibits greater stability under daylight than other fluorophores. Over the duration of 30 min, the intensities of curcumin and Aniline blue displayed negligible fluctuation and no statistically significant differences were observed (P value < 0.05). In contrast, Calcofluor

intensities experienced substantial fluctuation in the same 30 min intervals. The stability of curcumin aligns with the previous study that the efficient polymer ratio complex can shield the curcumin from light-induced degradation (Pecora et al., 2016).

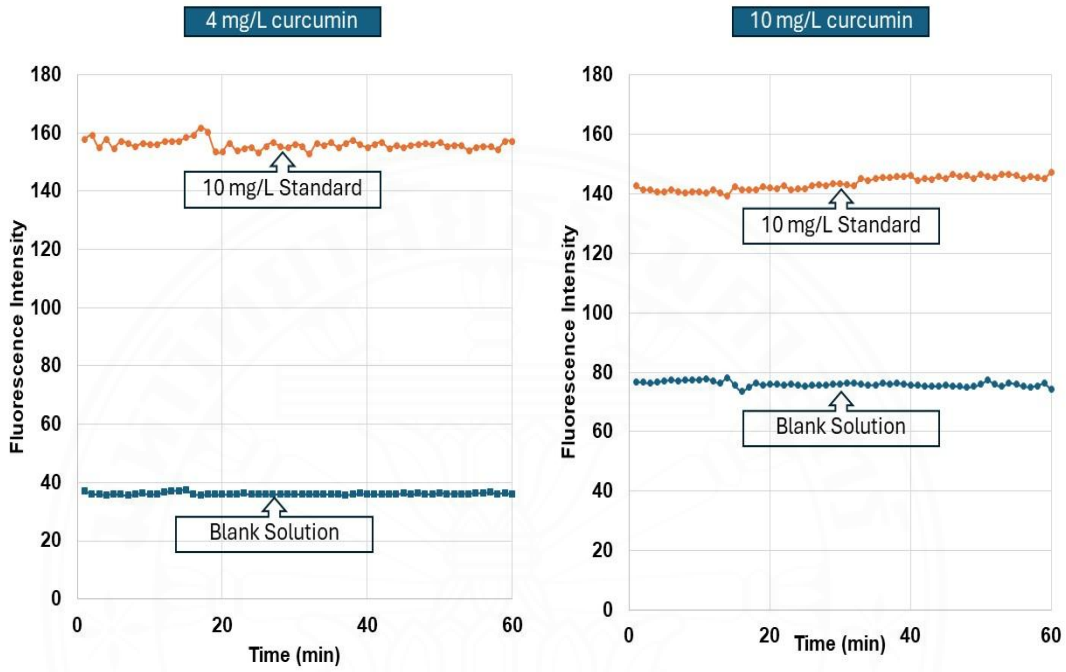

Figure 4.11 Stability of curcumin signal in both blank and standard solution (n=1).

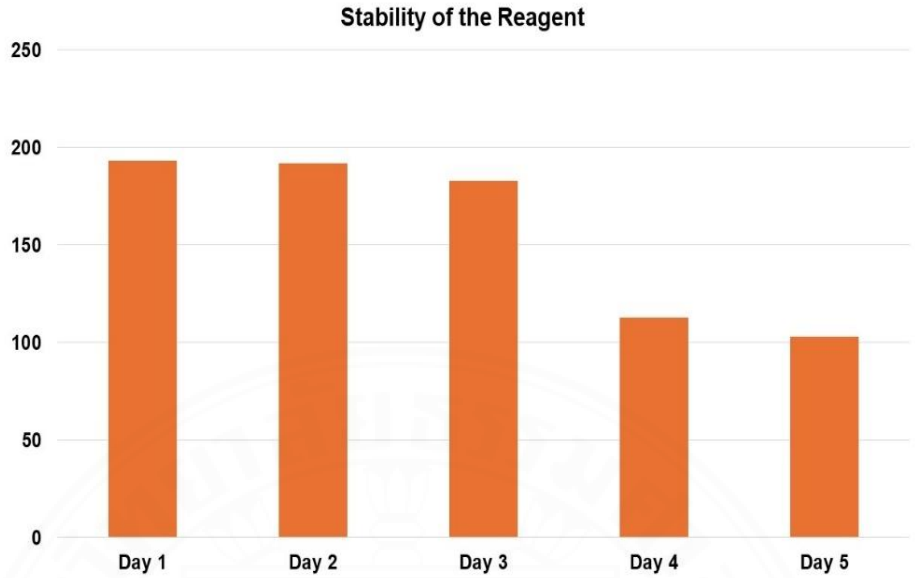

Figure 4.12 Investigation of reagent stability by measuring the mixture of curcumin and β-glucan for five consecutive days (n=3).

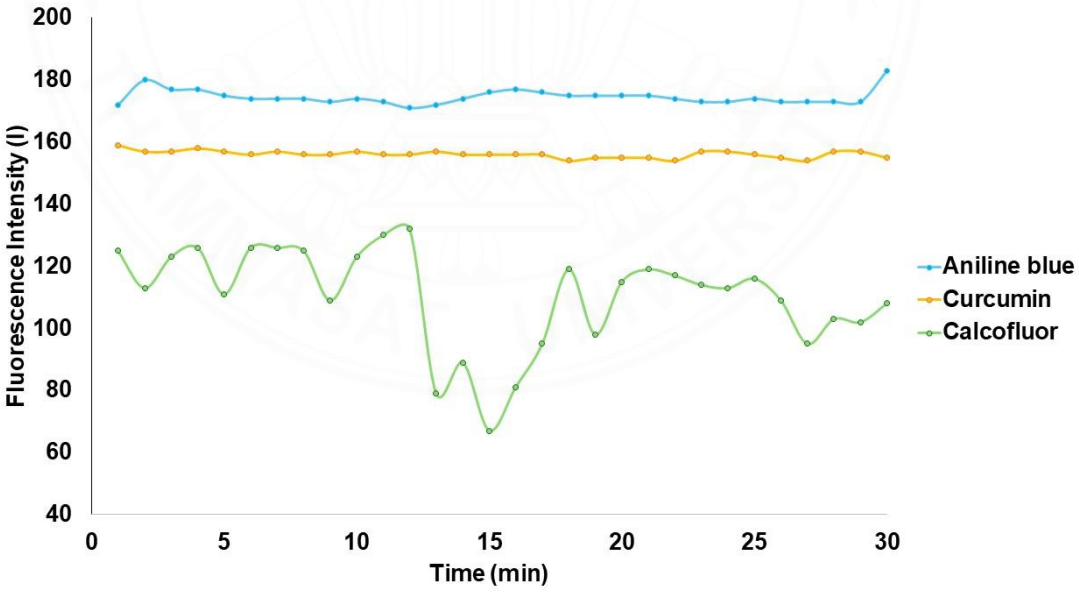

Figure 4.13 Light-sensitive nature of Aniline blue, Curcumin, and Calcofluor fluorophore after binding with β-glucan. The stability of the intensities was recorded over 30 min (n=1).

4.4 Analytical Method Validation

4.4.1 Linear Range

The linear range for the quantitative method was measured from 1 to 60 ppm of *β*-glucan standard solution plotted against increasing intensity. It was found that a lower concentration limit of *β*-glucan from 1 to 20 ppm correlates better with the lower amount of curcumin fluorophore 4 ppm. For higher concentrations of *β*-glucan from 20 to 70 ppm, the more concentrated curcumin unit of 10 ppm was used to establish the linear relationship. The high linear response was achieved through both concentrations of curcumin (4 and 10 ppm) of corresponding range evidence with the R-value of 0.99 as shown in Figures 3.7 & 3.8.

4.4.2 Precision analysis

The precision of the analytical method was conducted by measuring 3 concentration ranges in 3 times in compliance with the ICH (International Council for Harmonization) guidelines. The relative standard deviation was calculated as shown in Table 4.3. The proposed method provides high precision yielding an RSD value of < 2%.

Table 4.3 Precision analysis.

10 ppm Curcumin Concentration			4 ppm Curcumin Concentration		
Concentration	Intensity mean ± SD (n=3)	% RSD	Concentration	Intensity mean ± SD (n=3)	% RSD
20	245 ± 2.31	0.9	5	115.6 ± 0.55	0.48
40	358 ± 4.5	1.3	10	161.4 ± 1.82	1.13
60	404 ± 1.7	0.4	15	197 ± 1.58	0.8

4.4.3 LOD/LOQ

To get the LOD and LOQ value, the blank solution was measured ten times to have the average value and calculated with the slope of the intercept value. For 4 ppm curcumin concentration, LOD was 0.28 ppm and LOQ was 0.92 ppm. LOD and LOQ values for 20 ppm curcumin concentration were 1.5 ppm and 5 ppm respectively (Table 4.5).

4.4.4 Accuracy

The accuracy of the method was examined with standard additional by adding 10ppm of standard in eat mushroom samples extracts. The recovery for all samples fell within 90 to 110% and got excellent accuracy as in Table 4.4.

Table 4.4 Accuracy analysis for curcumin concentration of 4 and 10 ppm (a).

a). Curcumin concentration (4 ppm)					
Sample	Extraction Methods	Initial content in sample (ppm) mean ± SD; n=3	Added (ppm)	Amount found (ppm) mean ± SD; n=3	Recovery %
Lentinus squarrosulus	AE	5.9 ± 0.1	10	15.5 ± 0.06	96
	ME	4.7 ± 0.06	10	14.5 ± 0.1	98
	HWE	4.8 ± 0.06	10	14.3 ± 0.1	95
Lentinula edodes	AE	6.6 ± 0.12	10	15.9 ± 0.1	93
	ME	1.5 ± 0.16	10	12.3 ± 0.06	108
	HWE	4.8 ± 0.1	10	14.6 ± 0.06	98

Table 4.4 Accuracy analysis for curcumin concentration of 4 and 10 ppm (b). (cont.)

b). Curcumin concentration (10 ppm)					
Sample	Extraction Methods	Initial content in sample (ppm) mean ± SD; n=3	Added (ppm)	Amount found (ppm) mean ± SD; n=3	Recovery %
Lentinus squarrosulus	AE	N.D	30	29 ± 0.64	97
	ME	7.5 ± 0.6	30	37.6 ± 0.13	100
	HWE	ND	30	31 ± 0.6	103
Lentinula edodes	AE	N.D	30	31.3 ± 0.8	104
	ME	N.D	30	29.1 ± 0.4	97
	HWE	N.D	30	28.9 ± 0.8	96

Table 4.5 Analytical Merit.

Analytical Parameters	4 ppm curcumin concentration	10 ppm curcumin concentration
Linear Regression Equation	y = 5.1947x + 9.03	y = 2.04x + 25.2
Linear Range	1 to 20 ppm	20 to 60 ppm
Correlation Coefficient	0.99	0.99
Blank solution (mean ± SD)	0.48	1.03
LOD (mg/L)	0.28	1.5
LOQ (mg/L)	0.92	5
Precision (%RSD)	Intensity RSD < 2 %	
Accuracy (%Recovery)	93 to 108 %	

4.5 Comparison with existing Fluorescence Methods (Aniline Blue, Calcofluor)

The performance of the developed curcumin method was compared with aniline blue and calcofluor fluorescence assay in real sample analysis. A comparison was made by selecting two different types of mushrooms (Khon Khao, and Shiitake)

extracted by different extraction methods (AE, HWE, and ME). With a confidence level of 95%, it was found that no significant difference between the results obtained from three assays ($p > 0.05$) Table 4.6 & 4.7. It can be concluded that the developed curcumin method can effectively analyze β-glucan as previously studied fluorescence method.

Table 4.6 Comparison of the outcomes with traditional fluorescence methods. (mean ± SD), n=3

Samples	**Extraction Methods**	**Fluorescence Methods**		
		Curcumin (ppm)	**Aniline blue (ppm)**	**Calcofluor (ppm)**
Lentinus squarrosulus	AE	5.8 ± 0.05	5.3 ± 0.17	6.1 ± 0.43
	ME	10.6 ± 0.05	10.3 ± 0.2	11.1 ± 0.21
	HWE	14.8 ± 0.05	14.1 ± 0.2	14.1 ± 0.78
Lentinula edodes	AE	10.1 ± 0.11	10 ± 0.2	10.2 ± 0.43
	ME	8.7 ± 0.11	8.4 ± 0.07	6.98 ± 0.22
	HWE	12.6 ± 0.15	12.6 ± 0.13	11.65 ± 0.37
Linear Regression Equation		**y = 10.508x + 15.342**	**y = 15.703x - 11.544**	**y = 2.667x + 36.463**

Table 4.7 ANOVA analysis for the comparative variance of different fluorescence methods.

ANOVA: Single factor

Summary

Groups	**Count**	**Sum**	**Average**	**Variance**
Curcumin	6	62.6	10.43333	9.674667
Aniline blue	6	60.7	10.11667	9.645667
Calcofluor	6	60.13	10.02167	9.022017

Source of Variation	***SS***	***df***	***MS***	***F***	***P-value***	***F crit***
Between Groups	0.557544	2	0.278772	0.029508	0.97098	3.68232
Within Groups	141.7118	15	9.44745			
Total	142.2693	17				

CHAPTER 5
CHAPTER 6CONCLUSIONS AND RECOMMENDATIONS

5.1 Conclusion

In this study, the fluorescence quantification method to label mushroom *β*-glucan from extracts of *Lentinula edodes* and *Lentinulus squarrulusus* was successfully developed using the biocompatible and eco-friendly curcumin fluorophore. The reagent and sample preparation steps were considerably fast and easy, with the reaction developing within 1 to 3 min. Remarkably, the fluorescence intensity of the developed method can remain consistent for up to 1 hour and withstand light interferences. The resulting outcomes are compared to the existing fluorescence methods exhibiting good analytical performance. It can successfully be applied to detect the mushroom *β*-glucan extracts from different types of mushrooms demonstrating its versatility. The Curcumin-based method offers several advantages: it was more straightforward and rapid, reducing the complexity and time required for the analysis, and minimized light sensitivity. Moreover, using curcumin as a fluorophore greatly reduces the impacts of hazardous substances released into the environment. This innovative approach not only enhances the efficiency and reliability of *β*-glucan detection in mushrooms but also aligns with sustainable and environmentally friendly practices.

5.2 Recommendation

Since yeast samples do not dissolve well under current conditions, we cannot include yeast samples in the present research. If a way to solubilize the yeast samples is developed, it will be possible to test the developed method with yeast samples. Additionally, if the sample matrix of food products is studied and the method is modified accordingly, this method has the potential to be used in the food products industry with high throughput in the future. Testing with different molecular weight standards using developed method might be more beneficial to distinguish effectiveness in further studies. Furthermore, since curcumin has metal chelating properties, a study

of metal interferences should be included in future perspectives involving different sample matrices

REFERENCES

Ahmad, A., Anjum, F. M., Zahoor, T., Nawaz, H., & Dilshad, S. M. R. (2012). Beta glucan: a valuable functional ingredient in foods. *Critical Reviews in Food Science and Nutrition*, *52*(3), 201–212. https://doi.org/10.1080/10408398.2010.499806

Apostu, P. M., Nicolau, A. I., Mihociu, T. E., & Catană, L. (2017). Enzymatic Quantification of *β*-glucan in a Finely Comminuted Meat Product System. *Food Analytical Methods*, *10*(8), 2908–2912. https://doi.org/10.1007/s12161-017-0856-8

Bashir, K. M. I., & Choi, J. (2017). Clinical and Physiological perspectives of *β*-Glucans: the past, present, and future. *International Journal of Molecular Sciences*, *18*(9), 1906. https://doi.org/10.3390/ijms18091906

Bhatia, N. K., Kishor, S., Katyal, N., Gogoi, P., Narang, P., & Deep, S. (2016). Effect of pH and temperature on conformational equilibria and aggregation behaviour of curcumin in aqueous binary mixtures of ethanol. *RSC Advances*, *6*(105), 103275–103288. https://doi.org/10.1039/c6ra24256a

Boruah, B., Saikia, P. M., & Dutta, R. K. (2012). Binding and stabilization of curcumin by mixed chitosan–surfactant systems: A spectroscopic study. *Journal of Photochemistry and Photobiology. A, Chemistry*, *245*, 18–27. https://doi.org/10.1016/j.jphotochem.2012.07.004

Chan, G. C., Chan, W. K., & Sze, D. M. (2009). The effects of *β*-glucan on human immune and cancer cells. *Journal of Hematology & Oncology*, *2*(1). https://doi.org/10.1186/1756-8722-2-25

Chen, M., Du, Z., Zheng, X., Li, D., Zhou, R., & Zhang, K. (2018). Use of curcumin in diagnosis, prevention, and treatment of Alzheimer's disease. *Neural Regeneration Research/Neural Regeneration Research*, *13*(4), 742. https://doi.org/10.4103/1673-5374.230303

Chignell, C. F., Bilskj, P., Reszka, K. J., Motten, A. G., Sik, R. H., & Dahl, T. A. (1994). Spectral and Photochemical properties of curcumin. *Photochemistry and Photobiology*, *59*(3), 295–302. https://doi.org/10.1111/j.1751-1097.1994.tb05037.x

Colaço, M., Roquito, T., Costa, J. P., Cruz, M. T., & Borges, O. (2023). The effect of Curcumin-Loaded glucan nanoparticles on immune cells: Size as a critical quality attribute. *Pharmaceutics*, *15*(2), 623. https://doi.org/10.3390/pharmaceutics15020623

Danielson, M. E., Dauth, R., Elmasry, N. A., Langeslay, R. R., Magee, A. S., & Will, P. M. (2010). Enzymatic Method To Measure *β*-1-3-*β*-1-6-Glucan Content in Extracts and Formulated Products (GEM Assay). *Journal of Agricultural and Food Chemistry*, *58*(19), 10305–10308. https://doi.org/10.1021/jf102003m

Devasena, T., Balasubramanian, N., Muninathan, N., Baskaran, K., & John, S. T. (2022). Curcumin is an iconic ligand for detecting environmental pollutants. *Bioinorganic Chemistry and Applications/Bioinorganic Chemistry and Applications*, *2022*, 1–12. https://doi.org/10.1155/2022/9248988

Du, B., Bian, Z., & Xu, B. (2013). Skin Health Promotion Effects of Natural Beta-Glucan Derived from Cereals and Microorganisms: A Review. *PTR. Phytotherapy Research/Phytotherapy Research*, *28*(2), 159–166. https://doi.org/10.1002/ptr.4963

Erez, Y., Simkovitch, R., Shomer, S., Gepshtein, R., & Huppert, D. (2014). Effect of acid on the Ultraviolet-Visible absorption and emission properties of curcumin. ˜ *the œJournal of Physical Chemistry. A/the Journal of Physical Chemistry. A.*, *118*(5), 872–884. https://doi.org/10.1021/jp411686d

Fang, X., Zou, M., Chen, F., Ni, H., Nie, S., & Yin, J. (2021). An overview on interactions between natural product-derived *β*-glucan and small-molecule compounds. *Carbohydrate Polymers*, *261*, 117850. https://doi.org/10.1016/j.carbpol.2021.117850

Fu, D., Fu, J., Li, J., Tang, Y., Shao, Z., Zhou, D., & Song, L. (2022). Efficient encapsulation of curcumin into spent brewer's yeast using a pH-driven method. *Food Chemistry*, *394*, 133537. https://doi.org/10.1016/j.foodchem.2022.133537

Fu, Y., Lin, S., Lu, M., Wei, S., Zhou, J., Zhao, L., Zhang, Q., Lin, D., Liu, Y., Chen, H., Qin, W., & Wu, D. (2019). Quantitative Evaluation of Ultrasound-Assisted Extraction of 1-3-*β*-glucans from Dictyophora indusiata Using an Improved

Fluorometric Assay. *Polymers*, *11*(5), 864. https://doi.org/10.3390/polym11050864

Gao, Z., Hao, Y., Zheng, M., & Chen, Y. (2017). A fluorescent dye with large Stokes shift and high stability: synthesis and application to live cell imaging. *RSC Advances*, *7*(13), 7604–7609. https://doi.org/10.1039/c6ra27547h

Ghatak, C., Rao, V. G., Mandal, S., Ghosh, S., & Sarkar, N. (2012). An Understanding of the Modulation of Photophysical Properties of Curcumin inside a Micelle Formed by an Ionic Liquid: A New Possibility of Tunable Drug Delivery System. *the Journal of Physical Chemistry. B*, *116*(10), 3369–3379. https://doi.org/10.1021/jp211242c

Gil-Ramírez, A., Smiderle, F. R., Morales, D., Iacomini, M., & Soler-Rivas, C. (2019). Strengths and weaknesses of the aniline-blue method used to test mushroom (1→3)-*β*-d-glucans obtained by microwave-assisted extractions. *Carbohydrate Polymers*, *217*, 135–143. https://doi.org/10.1016/j.carbpol.2019.04.051

Gómez, C., Navarro, A., Carbonell, J., & Sendra, J. (2000). RESEARCH NOTE - Determination of the Apparent Molecular Weight Cut-off for the Fluorometric Calcofluor-FIA Method when Detecting (1→3),(1→4)-*β*-D-glucan using a High Ionic Strength Eluant. *Journal of Cereal Science*, *31*(2), 155–157. https://doi.org/10.1006/jcrs.1999.0247

Gao, Z., Hao, Y., Zheng, M., & Chen, Y. (2017). A fluorescent dye with large Stokes shift and high stability: synthesis and application to live cell imaging. *RSC Advances*, *7*(13), 7604–7609. https://doi.org/10.1039/c6ra27547h

Guo, Y., Yang, C., Zhang, Y., & Tao, T. (2022). Nanomaterials for fluorescent detection of curcumin. *Spectrochimica Acta. Part a, Molecular and Biomolecular Spectroscopy*, *265*, 120359. https://doi.org/10.1016/j.saa.2021.120359

Hammarström, H., Kondori, N., Friman, V., & Wennerås, C. (2015). How to interpret serum levels of beta-glucan for the diagnosis of invasive fungal infections in adult high-risk hematology patients: optimal cut-off levels and confounding factors. *European Journal of Clinical Microbiology & Infectious Diseases*, *34*(5), 917–925.

https://doi.org/10.1007/s10096-014-2302-9

Henry, R. J. (1984). A SIMPLIFIED ENZYMIC METHOD FOR THE DETERMINATION OF (1→3) (1→4)-*β*-GLUCANS IN BARLEY. *Journal of the Institute of Brewing*, *90*(3), 178–180. https://doi.org/10.1002/j.2050-0416.1984.tb04259.x

Howie, A. J. (2019). Origins of a pervasive, erroneous idea: The "green birefringence" of Congo red-stained amyloid. *International Journal of Experimental Pathology*, *100*(4), 208–221. https://doi.org/10.1111/iep.12330

Ide, M., Okumura, M., Koizumi, K., Kumagai, M., Yoshida, I., Yoshida, M., Mishima, T., & Nakamura, M. (2018). Novel method to quantify *β*-Glucan in processed foods: sodium hypochlorite extracting and enzymatic digesting (SEED) assay. *Journal of Agricultural and Food Chemistry*, *66*(4), 1033–1038. https://doi.org/10.1021/acs.jafc.7b05044

Izawa, M., Takashio, M., & Tamaki, T. (1996). INHIBITOR OF FLUORESCENCE REACTIONS BETWEEN CALCOFLUOR AND *β*-(1-3)(1,4)-D-GLUCAN IN BEER AND WORT. *Journal of the Institute of Brewing*, *102*(2), 87–91. https://doi.org/10.1002/j.2050-0416.1996.tb00898.x

Jagannathan, R., Abraham, P. M., & Poddar, P. (2012). Temperature-Dependent spectroscopic evidences of curcumin in aqueous medium: A Mechanistic study of its solubility and Stability. *the Journal of Physical Chemistry. B*, *116*(50), 14533–14540. https://doi.org/10.1021/jp3050516

Jin, Y., Li, P., & Wang, F. (2018). *β*-glucans as potential immunoadjuvants: A review on the adjuvanticity, structure-activity relationship and receptor recognition properties. *Vaccine*, *36*(35), 5235–5244. https://doi.org/10.1016/j.vaccine.2018.07.038

Jørgensen, K. G. (1983). An improved method for determining *β*-glucan in wort and beer by use of Calcofluor. *Carlsberg Research Communications*, *48*(5), 505–516. https://doi.org/10.1007/bf02908693

Karimi, M., Mashreghi, M., Saremi, S. S., & Jaafari, M. R. (2020). Spectrofluorometric method development and validation for the determination of curcumin in nanoliposomes and plasma. *Journal of Fluorescence*, *30*(5), 1113–1119. https://doi.org/10.1007/s10895-020-02574-3

Kharat, M., Du, Z., Zhang, G., & McClements, D. J. (2017). Physical and chemical stability of curcumin in aqueous solutions and emulsions: impact of pH, temperature, and molecular environment. *Journal of Agricultural and Food Chemistry*, *65*(8), 1525–1532. https://doi.org/10.1021/acs.jafc.6b04815

Khorasani, M. Y., Langari, H., Sany, S. B. T., Rezayi, M., & Sahebkar, A. (2019). The role of curcumin and its derivatives in sensory applications. *Materials Science & Engineering. C, Biomimetic Materials, Sensors and Systems*, *103*, 109792. https://doi.org/10.1016/j.msec.2019.109792

Kim, S., & Inglett, G. E. (2006). Molecular weight and ionic strength dependence of fluorescence intensity of the Calcofluor/*β*-glucan complex in flow-injection analysis. *Journal of Food Composition and Analysis*, *19*(5), 466–472. https://doi.org/10.1016/j.jfca.2005.11.006

Kim, S., Inglett, G. E., & Liu, S. X. (2008). Content and molecular weight Distribution of OaT *β*-Glucan in Oatrim, Nutrim, and C-Trim products. *Cereal Chemistry*, *85*(5), 701–705. https://doi.org/10.1094/cchem-85-5-0701

Ko, Y., & Lin, Y. (2004). 1-3- *β*-Glucan quantification by a fluorescence microassay and analysis of its distribution in foods. *Journal of Agricultural and Food Chemistry*, *52*(11), 3313–3318. https://doi.org/10.1021/jf0354085

Koenig, S., Rühmann, B., Sieber, V., & Schmid, J. (2017). Quantitative assay of *β*-(1-3)–*β*-(1-6)–glucans from fermentation broth using aniline blue. *Carbohydrate Polymers*, *174*, 57–64. https://doi.org/10.1016/j.carbpol.2017.06.047

Kotha, R. R., & Luthria, D. L. (2019). Curcumin: biological, pharmaceutical, nutraceutical, and analytical aspects. *Molecules/Molecules Online/Molecules Annual*, *24*(16), 2930. https://doi.org/10.3390/molecules24162930

Kumavat, S. D., Chaudhari, Y., Borole, P., & Duvvuri, P. (2013). Degradation studies of curcumin. *ResearchGate*. https://www.researchgate.net/publication/286451838_Degradation_studies_of_curcumin

Kupetz, M., Aumer, J., Harms, D., Zarnkow, M., Sacher, B., & Becker, T. (2016). High-throughput *β*-glucan analyses and their relationship with beer

filterability. *European Food Research & Technology*, *243*(2), 341–351. https://doi.org/10.1007/s00217-016-2748-3

Le, M. H., Doan, H., DO, Thi, H. H. T., Dung, L. V., Nguyen, H. N., Thi, H. N. T., Nguyen, L. D., Hoang, C. K., Le, H. C., Thi, T. H. L., Trinh, H. T., & Ha, P. T. (2016). The dual effect of curcumin nanoparticles encapsulated by 1-3/1-6 *β* -glucan from medicinal mushrooms Hericium erinaceus and Ganoderma lucidum. *Advances in Natural Sciences Nanoscience and Nanotechnology*, *7*(4), 045019. https://doi.org/10.1088/2043-6262/7/4/045019

Lendel, C., Bolognesi, B., Wahlström, A., Dobson, C. M., & Gräslund, A. (2010). Detergent-like Interaction of Congo Red with the Amyloid *β* Peptide. *Biochemistry*, *49*(7), 1358–1360. https://doi.org/10.1021/bi902005t

Li, H., Zhao, M., Zhou, S., Zhang, H., Wang, J., Xia, N., Liu, Y., Hua, S., & Tan, G. (2024). Enhancing encapsulation of curcumin by pH-driven and sodium alginate blending with ovalbumin as a carrier. *Food Hydrocolloids*, *149*, 109623. https://doi.org/10.1016/j.foodhyd.2023.109623

Liss, B., Cornely, O. A., Hoffmann, D., Dimitriou, V., & Wisplinghoff, H. (2015). 1-3-*β*-d-Glucan contamination of common antimicrobials: Table 1. *the Journal of Antimicrobial Chemotherapy/Journal of Antimicrobial Chemotherapy*, *71*(4), 913–915. https://doi.org/10.1093/jac/dkv419

Liu, Y., Zhang, C., Pan, H., Li, L., Yu, Y., & Liu, B. (2021). An insight into the in vivo imaging potential of curcumin analogues as fluorescence probes. *Asian Journal of Pharmaceutical Sciences*, *16*(4), 419–431. https://doi.org/10.1016/j.ajps.2020.11.003

Lowman, D. W., & Williams, D. L. (2001). A proton nuclear magnetic resonance method for the quantitative analysis on a dry weight basis of (1→3)-*β*-D-Glucans in a complex, Solvent-Wet matrix. *Journal of Agricultural and Food Chemistry*, *49*(9), 4188–4191. https://doi.org/10.1021/jf010435l

Mabrouk, M. M., Hamed, N. A., & Mansour, F. R. (2021). Simple spectrophotometric method to measure surfactant CMC by employing the optical properties of curcumin's tautomers. *Journal of Chemical Education*, *98*(8), 2603–2609.

https://doi.org/10.1021/acs.jchemed.1c00242

Madacsi, J. P., Parrish, F. W., & Roberts, E. J. (1983). Nonenzymic method for determination of Beta-Glucan in the presence of starch. *Journal of the American Society of Brewing Chemists*, *41*(4), 161–162. https://doi.org/10.1094/asbcj-41-0161

Magdy, G., Radwan, A. S., Belal, F., & El-Deen, A. K. (2023). Simple and affordable synchronous spectrofluorimetric determination of the natural anticancer polyphenols; resveratrol and curcumin in human plasma. *Spectrochimica Acta. Part a, Molecular and Biomolecular Spectroscopy*, *302*, 123029. https://doi.org/10.1016/j.saa.2023.123029

Manabe, N., & Yamaguchi, Y. (2021). 3D Structural Insights into *β*-Glucans and Their Binding Proteins. *International Journal of Molecular Sciences*, *22*(4), 1578. https://doi.org/10.3390/ijms22041578

Mcclear, B. V., & Glennie-Holmes, M. (1985). ENZYMIC QUANTIFICATION OF (1→3) (1→4)-*β*-D-GLUCAN IN BARLEY AND MALT. *Journal of the Institute of Brewing*, *91*(5), 285–295. https://doi.org/10.1002/j.2050-0416.1985.tb04345.x

McCleary, B. V., & Codd, R. (1991). Measurement of (1 → 3),(1 → 4)-*β*-D-glucan in barley and oats: A streamlined enzymic procedure. *Journal of the Science of Food and Agriculture/Journal of the Science of Food and Agriculture*, *55*(2), 303–312. https://doi.org/10.1002/jsfa.2740550215

Mekis, E., Pintér, G., & Béndek, G. (1987). Modified fluorometric flow-injection-analysis (FIA) method for the determination of (1-3) (1-4)-*β*-D-glucan. *Journal of the Institute of Brewing*, *93*(5), 396–398. https://doi.org/10.1002/j.2050-0416.1987.tb04525.x

Mohan, P. K., Sreelakshmi, G., Muraleedharan, C., & Joseph, R. (2012). Water soluble complexes of curcumin with cyclodextrins: Characterization by FT-Raman spectroscopy. Vibrational Spectroscopy, 62, 77–84. https://doi.org/10.1016/j.vibspec.2012.05.002

Mondal, S., Ghosh, S., & Moulik, S. P. (2016). Stability of curcumin in different solvent and solution media: UV–visible and steady-state fluorescence spectral

study. *Journal of Photochemistry and Photobiology. B, Biology*, *158*, 212–218. https://doi.org/10.1016/j.jphotobiol.2016.03.004

Morales, D., Rutckeviski, R., Villalva, M., Abreu, H., Soler-Rivas, C., Santoyo, S., Iacomini, M., & Smiderle, F. R. (2020). Isolation and comparison of α- and *β*-D-glucans from shiitake mushrooms (Lentinula edodes) with different biological activities. *Carbohydrate Polymers*, *229*, 115521. https://doi.org/10.1016/j.carbpol.2019.115521

Motilva, M., Serra, A., Borrás, X., Romero, M., Domínguez, A., Labrador, A., & Peiró, L. (2014). Adaptation of the standard enzymatic protocol (Megazyme method) to microplate format for *β*-(1-3)(1,4)-d-glucan determination in cereal based samples with a wide range of *β*-glucan content. *Journal of Cereal Science*, *59*(2), 224–227. https://doi.org/10.1016/j.jcs.2014.01.007

Nitschke, J., Modick, H., Busch, E., Von Rekowski, R. W., Altenbach, H., & Mölleken, H. (2011). A new colorimetric method to quantify *β*-1-3-1-6-glucans in comparison with total *β*-1-3-glucans in edible mushrooms. *Food Chemistry*, *127*(2), 791–796. https://doi.org/10.1016/j.foodchem.2010.12.149

Ogawa, K., Wanatabe, T., Tsurugi, J., & Ono, S. (1972). Conformational behavior of a gel-forming (1→3)-*β*-D-glucan in alkaline solution. *Carbohydrate Research*, *23*(3), 399–405. https://doi.org/10.1016/s0008-6215(00)82709-3

Pang, L., Zhou, Y., Gao, W., Zhang, J., Song, H., Wang, X., Wang, Y., & Peng, X. (2017). Curcumin-Based fluorescent and colorimetric probe for detecting cysteine in living cells and zebrafish. *Industrial & Engineering Chemistry Research*, *56*(27), 7650–7655. https://doi.org/10.1021/acs.iecr.7b02133

Patra, D., & Barakat, C. (2011). Synchronous fluorescence spectroscopic study of solvatochromic curcumin dye. *Spectrochimica Acta. Part a, Molecular and Biomolecular Spectroscopy*, *79*(5), 1034–1041. https://doi.org/10.1016/j.saa.2011.04.016

Patra, D., & Kurdi, R. E. (2021). Curcumin as a novel reducing and stabilizing agent for the green synthesis of metallic nanoparticles. *Green Chemistry Letters and Reviews*, *14*(3), 474–487. https://doi.org/10.1080/17518253.2021.1941306

Pecora, T. M., Cianciolo, S., Catalfo, A., De Guidi, G., Ruozi, B., Cristiano, M. C., Paolino, D., Graziano, A. C., Fresta, M., & Pignatello, R. (2016). Preparation, characterization and photostability assessment of curcumin microencapsulated within methacrylic copolymers. *Journal of Drug Delivery Science and Technology*, *33*, 88–97. https://doi.org/10.1016/j.jddst.2016.03.013

Peng, S., Li, Z., Zou, L., Liu, W., Liu, C., & McClements, D. J. (2018). Improving curcumin solubility and bioavailability by encapsulation in saponin-coated curcumin nanoparticles prepared using a simple pH-driven loading method. Food & Function, 9(3), 1829–1839. https://doi.org/10.1039/c7fo01814b

Pérez-Vendrell, A., Guasch, J., Francesch, M., Molina-Cano, J., & Brufau, J. (1995). Determination of *β*-(1–3), (1–4)-D-glucans in barley by reversed-phase high-performance liquid chromatography. *Journal of Chromatography a/Journal of Chromatography*, *718*(2), 291–297. https://doi.org/10.1016/0021-9673(95)00694-x

Plavcová, Z., Šalamúnová, P., Saloň, I., Štěpánek, F., Hanuš, J., & Hošek, J. (2019). Curcumin encapsulation in yeast glucan particles promotes its anti-inflammatory potential in vitro. *International Journal of Pharmaceutics*, *568*, 118532. https://doi.org/10.1016/j.ijpharm.2019.118532

Rieder, A., Knutsen, S. H., Ballance, S., Grimmer, S., & Airado-Rodríguez, D. (2012). Cereal *β*-glucan quantification with calcofluor-application to cell culture supernatants. *Carbohydrate Polymers*, *90*(4), 1564–1572. https://doi.org/10.1016/j.carbpol.2012.07.031

Rizkyana, A. D., Ho, T. C., Roy, V. C., Park, J., Kiddane, A. T., Kim, G., & Chun, B. (2022). Sulfation and characterization of polysaccharides from Oyster mushroom (Pleurotus ostreatus) extracted using subcritical water. *the Journal of Supercritical Fluids/the Journal of Supercritical Fluids*, *179*, 105412. https://doi.org/10.1016/j.supflu.2021.105412

Rotrekl, D., Šalamúnová, P., Paráková, L., Baďo, O., Saloň, I., Štěpánek, F., Hanuš, J., & Hošek, J. (2021). Composites of yeast glucan particles and curcumin lead to improvement of dextran sulfate sodium-induced acute bowel inflammation

in rats. *Carbohydrate Polymers*, *252*, 117142. https://doi.org/10.1016/j.carbpol.2020.117142

Šalamúnová, P., Saloň, I., Ruphuy, G., Kroupová, J., Balouch, M., Hanuš, J., & Štěpánek, F. (2021). Evaluation of *β*-glucan particles as dual-function carriers for poorly soluble drugs. *European Journal of Pharmaceutics and Biopharmaceutics*, *168*, 15–25. https://doi.org/10.1016/j.ejpb.2021.08.001

Schmitt, M. R., & Budde, A. D. (2009). Calcofluor fluorescence assay for Wort *β* -Glucan in a microplate format. *Cereal Chemistry*, *86*(1), 33–36. https://doi.org/10.1094/cchem-86-1-0033

Semedo, M. C., Karmali, A., & Fonseca, L. (2015). A high throughput colorimetric assay of β-1-3-d-glucans by Congo red dye. *Journal of Microbiological Methods*, *109*, 140–148. https://doi.org/10.1016/j.mimet.2014.12.020

Shaheen, T. I., Hussien, G. M., Mekawey, A. A., Ghalia, H., Youssry, A. A., & Mokadem, M. T. E. (2022). Facile extraction of nanosized *β*-glucans from edible mushrooms and their antitumor activities. *Journal of Food Composition and Analysis*, *111*, 104607. https://doi.org/10.1016/j.jfca.2022.104607

Tang, B., Ma, L., Wang, H., & Zhang, G. (2002). Study on the Supramolecular Interaction of Curcumin and *β*-cyclodextrin by Spectrophotometry and Its Analytical Application. *Journal of Agricultural and Food Chemistry*, *50*(6), 1355–1361. https://doi.org/10.1021/jf0111965

Theel, E. S., & Doern, C. D. (2013). Point-Counterpoint: *β*- d -Glucan Testing Is Important for Diagnosis of Invasive Fungal Infections. *Journal of Clinical Microbiology*, *51*(11), 3478–3483. https://doi.org/10.1128/jcm.01737-13

Valeur, B., & Berberan-Santos, M. N. (2012). Characteristics of fluorescence emission. *Molecular Fluorescence*, 53–74. https://doi.org/10.1002/9783527650002.ch3

Vetvicka, V., Vannucci, L., Sima, P., & Richter, J. (2019). Beta glucan: supplement or drug? From laboratory to clinical trials. *Molecules/Molecules Online/Molecules Annual*, *24*(7), 1251. https://doi.org/10.3390/molecules24071251

Veverka, M., Dubaj, T., Gallovič, J., Jorík, V., Veverková, E., Mičušík, M., & Šimon, P. (2014). Beta-glucan complexes with selected nutraceuticals: Synthesis, characterization, and stability. *Journal of Functional Foods*, *8*, 309–318. https://doi.org/10.1016/j.jff.2014.03.032

Wood, P. J. (1980). The Interaction of Direct Dyes with Water Soluble Substituted Celluloses and Cereal *β*-Glucans. *Industrial & Engineering Chemistry Product Research and Development*, *19*(1), 19–23. https://doi.org/10.1021/i360073a006

Wu, C., Scott, J., & Shea, J. (2012). Binding of Congo Red to amyloid protofibrils of the Alzheimer AB9–40 peptide probed by molecular dynamics simulations. *Biophysical Journal*, *103*(3), 550–557. https://doi.org/10.1016/j.bpj.2012.07.008

Wu, J., Deng, X., Tian, B., Wang, L., & Xie, B. (2008). Interactions between Oat *β*-Glucan and Calcofluor Characterized by Spectroscopic Method. *Journal of Agricultural and Food Chemistry*, *56*(3), 1131–1137. https://doi.org/10.1021/jf072727d

Wulandari, A., Sunarti, T. C., Fahma, F., & Enomae, T. (2020). The potential of bioactives as biosensors for detection of pH. *IOP Conference Series. Earth and Environmental Science*, *460*(1), 012034. https://doi.org/10.1088/1755-1315/460/1/012034

Yakupova, E. I., Bobyleva, L. G., Vikhlyantsev, I. M., & Bobylev, A. G. (2019). Congo Red and amyloids: history and relationship. *Bioscience Reports*, *39*(1). https://doi.org/10.1042/bsr20181415

Zhan, X., Dai, L., Zhang, L., & Gao, Y. (2020). Entrapment of curcumin in whey protein isolate and zein composite nanoparticles using pH-driven method. *Food Hydrocolloids*, *106*, 105839. https://doi.org/10.1016/j.foodhyd.2020.105839

Zhong, W., Zhang, T., Dong, C., Li, J., Dai, J., & Wang, C. (2022). Effect of sodium chloride on formation and structure of whey protein isolate/hyaluronic acid complex and its ability to loading curcumin. *Colloids and Surfaces. A, Physicochemical and Engineering Aspects*, *632*, 127828. https://doi.org/10.1016/j.colsurfa.2021.127828

Zhu, F., Du, B., Bian, Z., & Xu, B. (2015). Beta-glucans from edible and medicinal mushrooms: Characteristics, physicochemical and biological activities. *Journal of Food Composition and Analysis*, *41*, 165–173. https://doi.org/10.1016/j.jfca.2015.01.019

Zsila, F., Bikádi, Z., & Simonyi, M. (2004). Circular dichroism spectroscopic studies reveal pH dependent binding of curcumin in the minor groove of natural and synthetic nucleic acids. *Organic & Biomolecular Chemistry*, *2*(20), 2902–2910. https://doi.org/10.1039/b409724f

BIOGRAPHY

Name	Pwint Phyu Theint
Educational Attainment	2023: Master's of Science (Chemistry)
Scholarship	Year 2023: Thammasat International Student Recruitment (TISR) Contract No. TB 2/2565
Proceeding	Development of an analytical fluorescence method for quantifying β-glucan content from mushroom extracts; utilizing curcumin as a green chemical fluorophore.